VŠB – Technical University of Ostrava

University Study Programme

Department of Control Systems and Instrumentation

Active Parametric Vibration Control of Dynamic Systems

Aktivní parametrické řízení vibrací dynamických systémů

Student: Bc. Radek Štramberský
Supervisor: prof. Ing. Jiří Tůma, CSc.

Ostrava 2019

VŠB - Technical University of Ostrava
University Study Programmes
Department of Control Systems and Instrumentation

Diploma Thesis Assignment

Student: **Bc. Radek Štramberský**

Study Programme: N3943 Mechatronics

Study Branch: 3906T006 Mechatronic Systems

Title: Active Parametric Vibration Control of Dynamic Systems
Aktivní parametrické řízení vibrací dynamických systémů

The thesis language: English

Description:

1. Create a simulation model of your test rig.
2. Define parameters marked "Principle and Combination Parametric Resonances" at resonant frequencies of the mechanical system and determine at which resonant frequency the highest damping effect is obtained.
3. Evaluate the effect of parametric vibration damping on the vibration magnitude at the resonant frequency with the use of experiment and simulation.
4. Evaluate the achieved results.

References:

TONDL, Aleš. Quenching of self-excited vibrations. Prague: Academia, 1991. ISBN 8020003428 9788020003423 0444987215 9780444987211.
TONDL, Aleš a Ladislav PŮST. To the Parametric Anti-Resonance Application. Engineering Mechanics: International Journal for Theoretical and Applied Mechanics. Association for Engineering Mechanics, 2010, 17, 2010(No. 2), pp. 135-144. ISSN 1802-1484.
TŮMA, Jiří, Pavel ŠURÁNEK a Miroslav MAHDAL. Vibration damping of the cantilever beam with the use of the parametric excitation. In: CROCKER, Malcolm J., Marek PAWELCZYK a Jing TIAN. 21st International Congress on Sound and Vibration (ICSV21), Beijing, China, 13-17 July 2014. Beijing: International Institute of Acoustics and Vibration (IIAV), 2014, s. 8. ISBN 978-83-62652-66-2. ISSN 2329-3675.
GHANDCHI, Tehrani M. a M.K. KALKOWSKI. Active control of parametrically excited systems. Intelligent Material Systems and Structures. 2016, 27(No. 9), 28. DOI: 10.1177/1045389X15588625. ISSN 1045-389X.

Extent and terms of a thesis are specified in directions for its elaboration that are opened to the public on the web sites of the faculty.

Supervisor: **prof. Ing. Jiří Tůma, CSc.**

Date of issue: 21.12.2018
Date of submission: 20.05.2019

VYSOKÁ ŠKOLA BÁŇSKÁ - TECHNICKÁ UNIVERZITA OSTRAVA UNIVERZITNÍ STUDIJNÍ PROGRAMY

doc. Ing. Renata Wagnerová, Ph.D.
Head of Department

Ing. Zdeňka Chmelíková, Ph.D.
Vice-rectress for Study Affairs

I hereby declare that this diploma thesis was written by myself. I have quoted all the references I have drawn upon.

Ostrava, May 20th 2019 .....

I declare that:

- I am aware that Act No. 121/2000 Coll., Act on copyright, rights related to copyright and amending some laws (the Copyright Act), in particular Section 35 (Use of a work in the civil or religious ceremonies or in official events organized by public authorities, in the context of university performance and use of university work) and Section 60 (university work) shall apply to my final Diploma thesis.
- I understand that VŠB – Technical University of Ostrava (hereinafter referred to as "VŠB-TUO") has the right to use this final Diploma thesis noncommercially for its internal use (Section 35 Subsection 3 of the Copyright Act)
- if requested, a copy of this Diploma thesis will be deposited with the thesis supervisor,
- if VŠB-TUO is interested, I will make a licensing agreement with it permitting to use the thesis within the scope of Section 12 Subsection 4 of the Copyright Act,
- I can only use my thesis, or grant a license to use it with the consent of VŠBTUO, which is authorized in such a case to demand an appropriate contribution to the costs that were incurred by VŠB-TUO to create the thesis (up to the actual amount),
- I understand that - according to Act No. 111/1998 Coll., on higher education institutions and on changes and amendments to other acts (Higher Education Act), as amended - that this Diploma the thesis will be available for public before the defence at the thesis supervisor's workplace, and electronically stored and published after the defence at the Central Library of VŠB-TUO, regardless of the outcome of its defence.

In Ostrava on May 20, 2019

.....

Signature of the author

Name and surname of the thesis author: Radek Štramberský

Permanent address of the thesis author: Poruba 12, 753 66 Hustopeče nad Bečvou, Czechia

Abstract

ŠTRAMBERSKÝ R. Active Parametric Vibration Control of Dynamic Systems Type : Diploma Thesis. Ostrava: VŠB – Technical University of Ostrava, University study programmes, Department of Control Systems and Instrumentation, 2016, 69 s. Supervisor: Tůma, J.

Parametric excitation can usually be seen in the large mechanical structure causing unwanted resonances when the static parameters of the system change usually by vibrations. In this work, we discuss the non-linear properties like stability and damping effect of the periodic change of the system's stiffness. Parametric excitation is added into the system by using negative position feedback with parametric gain change. Test rig of a cantilever beam with piezoelectric actuator and sensor is used, the identification and then simulation is made the same as practical measurements. Fixed end of cantilever bean is kinematically excited while combination parametric resonance is used for active vibration damping.

Keywords: active vibration control, damped mathieu equation, principle parametric resonance, combination parametric resonance, piezoelectric actuators

Abstrakt

ŠTRAMBERSKÝ R. Aktivní parametrické řízení vibrací dynamických systémů : diplomová práce. Ostrava: VŠB - Technická univerzita Ostrava, Univerzitní studijní programy, Katedra automatizační techniky a řízení, 2019, 69 s. Vedoucí: Tůma, J.

Parametrické buzení lze obvykle pozorovat u velkých mechanických struktur, kde způsobuje nežádoucí rezonance, když se statické parametry systému mění (obvykle vibracemi). V této práci se zabýváme nelineárními vlastnostmi, jako je stabilita a tlumící účinek periodické změny tuhosti systému. Parametrická excitace je přidána do systému pomocí záporné zpětné vazby polohy s parametrickou změnou zesílení. Je použito zkušební zařízení ukotveného nosníku s piezoelektrickým pohonem a senzorem. Identifikace a poté simulace se provádí stejně jako praktická měření kdy pevný konec ukotveného nosníku je kinematicky excitován a kombinační parametrická rezonance je využita pro aktivní tlumení vibrací.

Klíčové slova: aktivní tlumení vibrací, řízení vibrací, tlumená mathieova rovnice, principiální parametrická rezonance, kombinační parametrická rezonance, piezoelektrické aktuátory

Contents

List of symbols and abbreviations

AVC	–	Active Vibration Control
DoF	–	Degree of Freedom
FFT	–	Fast Fourier Transform
HIL	–	Hardware in the Loop
MSE	–	Mean Squared Error
PSD	–	Power Spectral Density
RMS	–	Root Mean Squere
A	–	Amplitude of periodic signal
$\mathbf{A}$	–	State (or system) matrix
b	–	Damping of the system
$\mathbf{B}$	–	Input matrix
BW	–	Correcting bandwidth based on used time window
$\mathbf{c^T}$	–	Output matrix
$\mathbf{d}$	–	Feedthrough (or feedforward) matrix
$e(t)$	–	Control error function
f_s	–	Sampling frequency
k	–	Stiffness of the system, index of the component
k_p	–	Proportional Gain PID parameter
K	–	System gain
m	–	Body mass
N	–	Number of samples used for FFT
r_{-1}	–	Integration independent parameter
r_0	–	Proportional independent parameter
r_1	–	Derivation independent parameter
ref	–	Reference value for dB scaling
t	–	Time variable
T_0	–	System time constant
T_D	–	Derivation Time PID parameter
T_I	–	Integration Time PID parameter
$u(t)$	–	Manipulated variable function
$\mathbf{u}(t)$	–	Input (or control) vector
$v(t)$	–	Disturbance variable function
$w(t)$	–	Command variable function
$x(t)$	–	Function of body displacement
x_0	–	Reference displacement
$\dot{x}(t)$	–	Derivation of displacement (velocity)

$\ddot{x}(t)$	–	Second Derivation of displacement (acceleration)
$\mathbf{x}(t)$	–	State vector
X	–	FFT image
$y(t)$	–	Controlled variable function
$\mathbf{y}(t)$	–	Output vector
ξ	–	System damping ratio
ω_n	–	Natural frequency
ω_p	–	Parametric resonance frequency (type not specified)
ω_n^{Cr}	–	Combination parametric resonances
ω_n^{Pr}	–	Principal parametric resonances

1 Introduction

In this introductory chapter we are going to describe for understanding the rest of the document and give the reader an idea about the motivation for this research topic.

1.1 Dynamic Systems Simulation

As stated in (Noskievič 1992), the dynamic system is a set of elements and relationships between them with certain properties with variable states.

In real life application, few different types of these systems are recognized: Mechanic, electric, pneumatic, hydraulic, thermal or their combination systems. Usually, it is common practice to simplify these real complex systems by modeling lumped parameter models with three basic parameters- stiffness (modeled as spring), mass (modeled as resistance) and damping (modeled as damper). (Noskievič 2013) The advantage of this approach is that there is a duality between these systems and therefore the usage of the same standardized tools is possible. Usually, these parameters are almost linear or we linearize them near a small working area. Working with linear systems allows us to simplify our problem and build robust predictable systems. In this thesis, we are going to assume that one of these parameters is not constant but change periodically. More about this problem will be described later.

Testing and development of the various application can cost a huge amount of resources. Building real devices and testing states and effect as resonance is very often not possible because of the risk of damaging expensive tools and devices. For making this test possible the computer simulation is an effective tool to study these systems before creating real applications.

1.2 Active Vibration Control

Vibrations are present in all applications and therefore it is important to test the application's behavior on different excitation frequencies. Resonances in the system can be destructive or cause malfunctions.

The purpose of vibration control is either to displace or reduce the amplitudes of resonant peaks. A couple of option to handle vibrations are available - isolate the system from the origin of

vibrations, make system stiffer or dampen the vibrations. Mechanical vibration can be damped passively or actively. (Šuránek 2016)

Active vibration control (AVC) are methods which use actuators acting on the system controlled by input which depends on feedback from sensors which measure the vibrations. The common practice is to dampen the vibration by using velocity feedback which add more damping into the system. Mechanical systems' damping ratio is usually very small. Another option is the usage of position feedback where the resonance peak is moved into another frequency. In this project, focus is on a different approach - using the parametric excitation. Mostly the mechanical systems are discussed but because of duality, these principles are present for all kind of the systems.

1.3 Piezoelectric Actuators and Sensors

For Active Vibration Control of Mechanical Dynamic systems, fast response actuators are needed. For Mechanical Dynamic Systems Magnetorheological fluids, Magnetic or piezoelectric actuators can be used. Using Magnetorheological fluid actuators for this purpose have an advantage of directly affecting the change of the stiffness. Because of the cost and easy to install properties of piezoelectric actuators, we are using these actuators.

"Piezoelectric Effect is the ability of certain materials to generate an electric charge in response to applied mechanical stress." (NANOMOTION)

"One of the unique characteristics of the piezoelectric effect is that it is reversible, meaning that materials exhibiting the direct piezoelectric effect (the generation of electricity when stress is applied) also exhibit the converse piezoelectric effect (the generation of stress when an electric field is applied)." (NANOMOTION)

A disadvantage of these actuators can be the force dependence on displacement. The advantage is easy to control, cheap and very fast response solution.

For this project, the Piezoactuators from company MIDÉ has been used (MIDÉ 2016).

1.4 Parametric Excitation

As stated before, the parametric excitation effect is based on periodically changing a parameter (stiffness, inertia or damping). Parametric change of one of these properties can be beneficial but also could bring the instabilities into the system. While the linear system can be only stable or unstable, the response of the nonlinear system depends also on the actual system variables' position and can be stable or unstable on more places at the state plane. There are real-life situations where modeling non-linearity is mandatory to ensure proper operation. For example, large mechanical structures where the different resonant frequencies could excite other parts by changing the stiffness of these parts on parametric resonant frequency like bridges or space applications.

In this work, the focus is on parametric principle and combination resonances. Even if the linear stability rules are respected, real systems are not usually linear and small change in one parameter can create big oscillations. In mechanical structures design, we can encounter such situations for example by looking at large space structures, plane's wings or bridges. In these examples, the stiffness of the system is usually changed periodically by different natural frequencies of the mechanism's parts. Even a small force can create a big displacement on these frequencies due to instability. (Ghandchi and Kalkowski 2016)

In this work, we want to change the stiffness not passively but actively by using piezo actuators of patch type. These actuators can change the stiffness of the system by applying torque to the beam. The position feedback is then used while the gain is periodically changed on combination parametric resonance frequency. (Tondl 2000)

Using this approach usage of this excitation to reduce main resonance peak into two smaller is wanted. This approach is often used for tall buildings, where near roof the pendulum is added. (Abe 2013)

1.5 Application fields

Even that most of the time we discuss mechanical structures, these effects exist in all kind of non-mechanical systems. Huge applications are in Civil engineering where passive equations are calculated to make sure that parametric resonance will not happen. Also tuned pendulums are used for tall buildings to dampen the first mode resonance.

Another usage is found in damping ship movement on the ocean where passive or active tanks are used or in planes' wings or for space structures.

Commonly used solutions are usually linear based simple systems which are robust and stable. For linear Mechanical and Electric systems, the stability condition is always fulfilled (Inertia, Stiffness, and Damping in Lumped Models are usually positive). Of course, the resonance effect (Which is considered as a stable state.) can cause destruction or malfunctions. If one of the parameters is not constant but change periodically, new resonant (unstable) regions are present. Because the system in these states is unstable, even small amplitude can cause huge displacement.

A disadvantage of this approach is higher complexity of the system but with enough knowledge, even better AVC solution design then by using conventional approaches is possible.

2 History and similar research

As stated before, research in vibration control field is nowadays very important and all science institutions invest their resources to study this field. For the diagnostic and optimization of current systems, this field is a requirement. This thesis would never be possible without their collaborations and publications. Therefore this chapter can be used as a source for more insight into the problem but also as a tool to show reader our expectation of results.

The main motivation for this research can be found in (Tondl 2000). As stated in picture 2.1, in multi-degree of freedom systems there are combination parametric frequencies which can be used for vibration damping. Prof. A. Tondl and Prof. F. Dohnal created the fundamentals in the field of Parametric excitation usage for damping (Dohnal and Tondl 2013), (Dohnal 2008a), (Dohnal 2008b).

A disadvantage of this approach is higher complexity of the system but with enough knowledge, we can create even better AVC solution then by using conventional approaches.

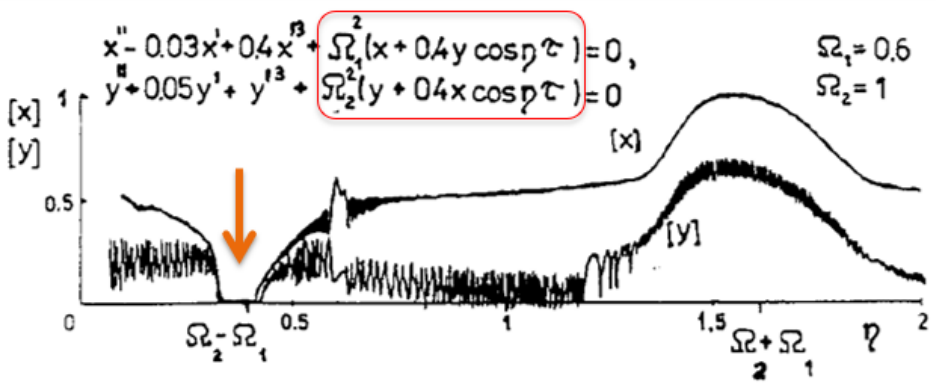

Figure 2.1: Effect of combination parametric resonances from (Tondl 2000)

This thesis is based on work made at the Department of Control Systems and Instrumentation on our university (VŠB - Technical University of Ostrava) mostly guided by Prof. Tůma. Few important sources will be highlighted now.

This project is a continuation of work "Active vibration control with the use of piezo actuators of patch type" (Štramberský 2016), which topic is the problem of linear vibration damping. The same piezoelectric actuators, dSpace controller, sensors are used for proving the physical applicability of this approach. Also in this work, the important input-output filtering is described.

A huge summary of linear AVC of linear systems which is used as a foundation for this thesis can be found in work "Active Vibration Damping" (Šuránek 2016).

Another very similar research to this thesis can be found in publication (Tůma et al. 2014a). In that research, the application is simulated on cantilever beam the same as in this thesis. Nonetheless few differences are present- In this thesis, the stability is described more deeply and as an actuator, the piezoelectric actuators are used which do not act on the system with point force but torque. Also, the content of the article is only simulation and results are not shown on the real physical application. Their model can be seen in 2.2.

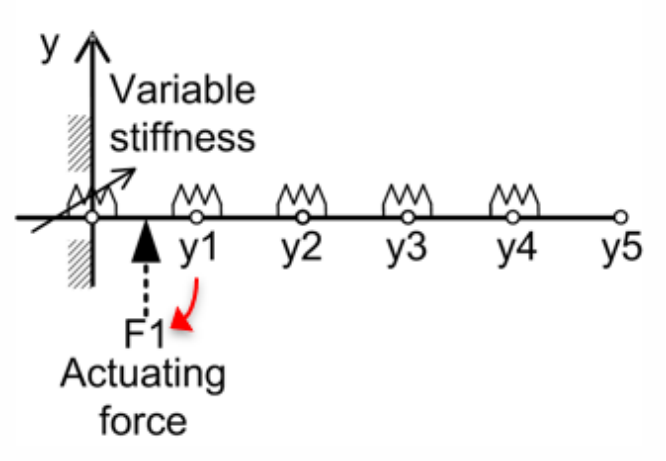

Figure 2.2: Lumped Parameter Model of cantilever beam from (Tůma et al. 2014a)

Their result is strong vibration damping on first natural frequency peak (which is split into two smaller peaks) while creating a new peak in higher frequency spectrum as plotted in 2.3.

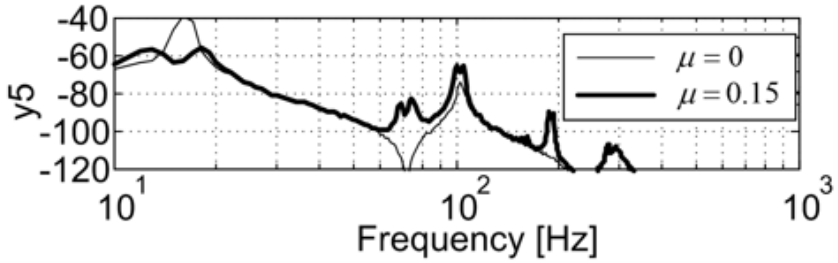

Figure 2.3: Lumped Parameter Model of cantilever beam from (Tůma et al. 2014a)

Another usage of parametric control was made in (Abe 2013) where an object's displacement on the pendulum is controlled by the change of pendulum's cable length.

Also the publication (Ghandchi and Kalkowski 2016) is taken as a foundation for creating this thesis where the stability problem is well described.

3 Single Degree of Freedom Systems

Before we move to our application of exploring parametric excitation for our cantilever beam, we will research a simple Single Degree of Freedom System.

3.1 Parametric Excitation by controller's gain periodic change

Let's assume the simple second-order mechanical system with lumped parameters - mass inertia, damper and spring (Noskievič 2013) as you can see in Figure 3.1.

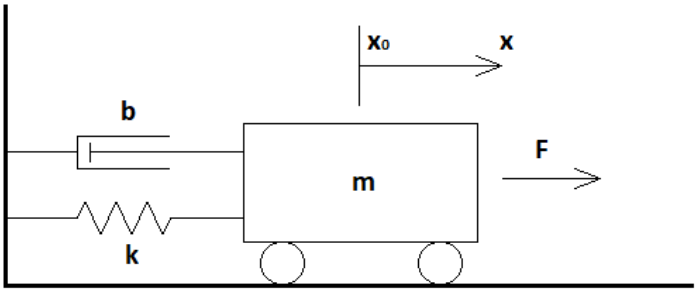

Figure 3.1: Mechanical lumped parameter model with one degree of freedom

The motion equation of this system is:

$$m \cdot \ddot{x}(t) = F(t) - b \cdot \dot{x}(t) - k \cdot x(t) \tag{3.1}$$

, where:
m is the body's mass,
t is time variable,
$x(t)$ is the function of body's displacement,
$F(t)$ is the function of the force acting on the body,
b is the damping,
k is the stiffness of the system.

After the substitution:

$$K = \frac{1}{k} \tag{3.2}$$

$$T_0 = \sqrt{\frac{m}{k}} \tag{3.3}$$

$$\xi = \frac{b}{2\sqrt{km}} \tag{3.4}$$

$$F(t) = v(t) + u(t) \tag{3.5}$$

, where:
K is system's gain,
T_0 is system's time constant,
ξ is system's damping ratio,
$v(t)$ is disturbance variable function,
$u(t)$ is manipulated variable function,
we receive the general second order equation 3.6.

$$T_0^2 \cdot \ddot{x}(t) = K \cdot (v(t) + u(t)) - 2T_0\xi \cdot \dot{x}(t) - x(t) \tag{3.6}$$

The general PID controller of this system has the equation 3.7.

$$u(t) = k_p \cdot \left(e(t) + T_D \cdot \dot{e}(t) + \frac{1}{T_I} \cdot \int e(t)dt\right) = r_0 \cdot \left(e(t) + \frac{r_1}{r_0} \cdot \dot{e}(t) + \frac{1}{\frac{r_0}{r_{-1}}} \cdot \int e(t)dt\right) \tag{3.7}$$

For studying properties of this system lets assume the autonomous system- the system without excitation.

$$v(t) = 0 \tag{3.8}$$

$$w(t) = \dot{x}^*(t) = 0 \tag{3.9}$$

$$y(t) = \dot{x}(t) \tag{3.10}$$

therefor:

$$e(t) = w(t) - y(t) = -\dot{x}(t) \tag{3.11}$$

, where:
$e(t)$ is the control error's function,
$y(t)$ is the controlled variable's function,

$w(t)$ is the command variable's function.

The equation 3.7 change into:

$$u(t) = -r_0 \cdot \dot{x}(t) - r_1 \cdot \ddot{x}(t) - \frac{1}{r_{-1}} \cdot x(t) \tag{3.12}$$

You can see this system's control circuit in Figure 3.2.

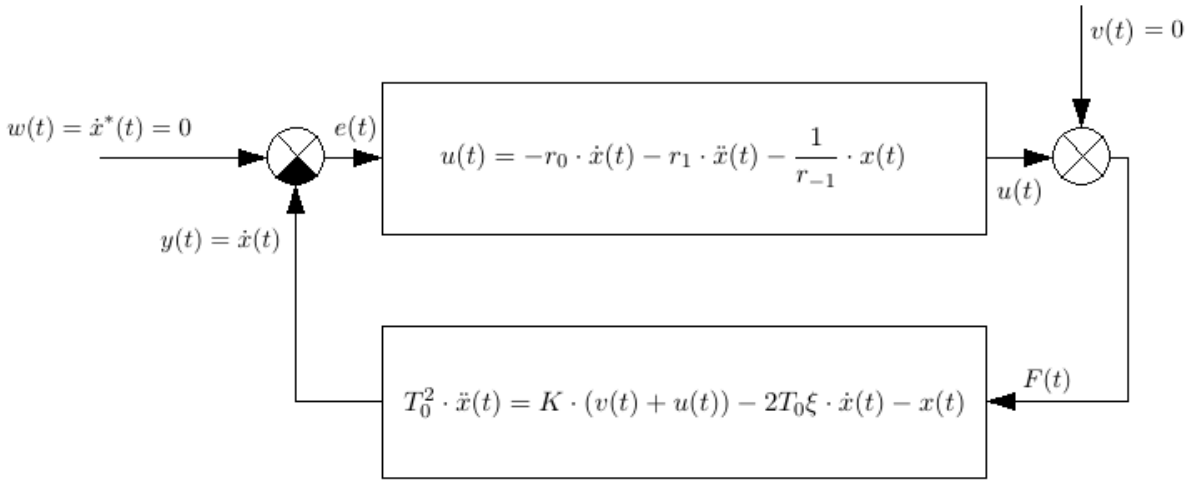

Figure 3.2: Control circuit for oscillation's stabilization

Now we can write the differential equation of such a system:

$$(T_0^2 + K \cdot r_1) \cdot \ddot{x}(t) + (K \cdot r_0 + 2T_0\xi) \cdot \dot{x}(t) + (K \cdot \frac{1}{r_{-1}} + 1) \cdot x(t) = 0 \tag{3.13}$$

As stated before, we are going to use position feedback so in our case:

$$r_1 = 0 \tag{3.14}$$

$$r_0 = 0 \tag{3.15}$$

After substitution:

$$\omega_n = \frac{1}{T_0} \tag{3.16}$$

, where ω_n is natural frequency of the system in radians.

We can edit our equation into:

$$\ddot{x}(t) + 2\omega_n\xi \cdot \dot{x}(t) + \omega_n^2 \cdot (K \cdot \frac{1}{r_{-1}} + 1) \cdot x(t) = 0 \tag{3.17}$$

As stated before, we want to parametrically excite the system. Our gain can have the infinity harmonic components described with the Fourier series:

$$\frac{1}{r_{-1}} = \sum_{n=0}^{\infty} A_n \cdot \cos n\omega_p t + B_n \cdot \sin n\omega_p t = \sum_{n=0}^{\infty} A_n \cdot \cos\left(n\omega_p t + n\phi_0\right) \tag{3.18}$$

Lets continue with simple parametrically excited system ($n_{max} = 1$). After the substitution:

$$K_0 = A_0 + K \tag{3.19}$$

$$\Delta K = A_1 \tag{3.20}$$

We receive:

$$\ddot{x}(t) + 2\omega_n\xi \cdot \dot{x}(t) + \omega_n^2 \cdot (K_0 + 1 + \Delta K \cdot \cos(\omega_p t)) \cdot x(t) = 0 \tag{3.21}$$

, which is well known form of Damped Mathieu equation. Control circuit can be seen in Figure 3.3.

3.2 Principle Parametric Resonances

When we talk about the stability of the system seen in equation 3.21 we can notice that if $\Delta K = 0$, all of the parameters will always be positive for the mechanical system. As known from control system theory, for second-order systems there is Stodola's sufficient condition, which says that if all the coefficient positive, the linear system is also positive.

The objects of our interest are systems with low damping ratio ($\xi < 1$). Linear system for $\Delta K = 0$ can be seen in Figure 3.4. The system is always stable and the velocity and position in the $t = \infty$ equals to zero.

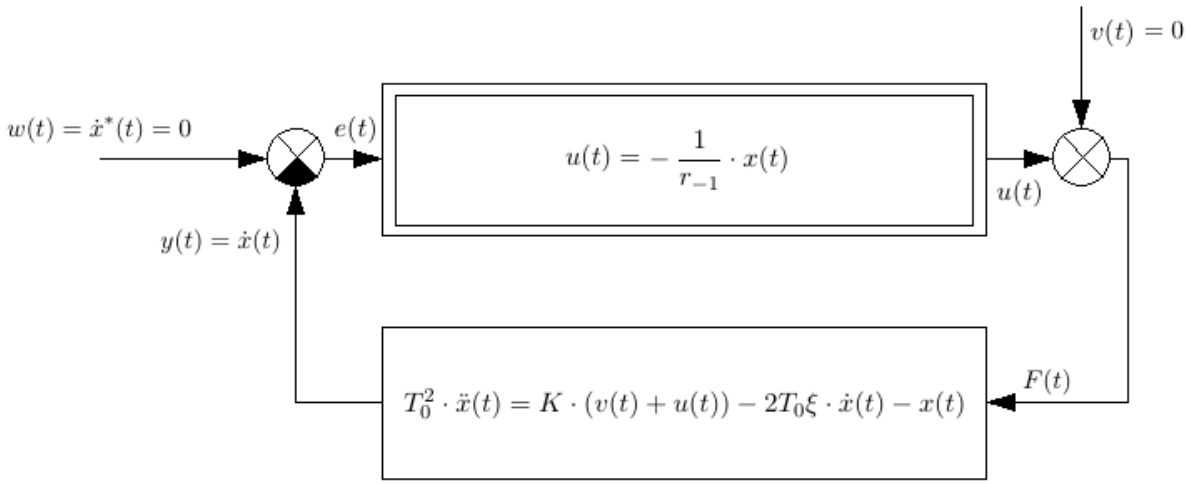

Figure 3.3: Control circuit for Damped Mathieu equation

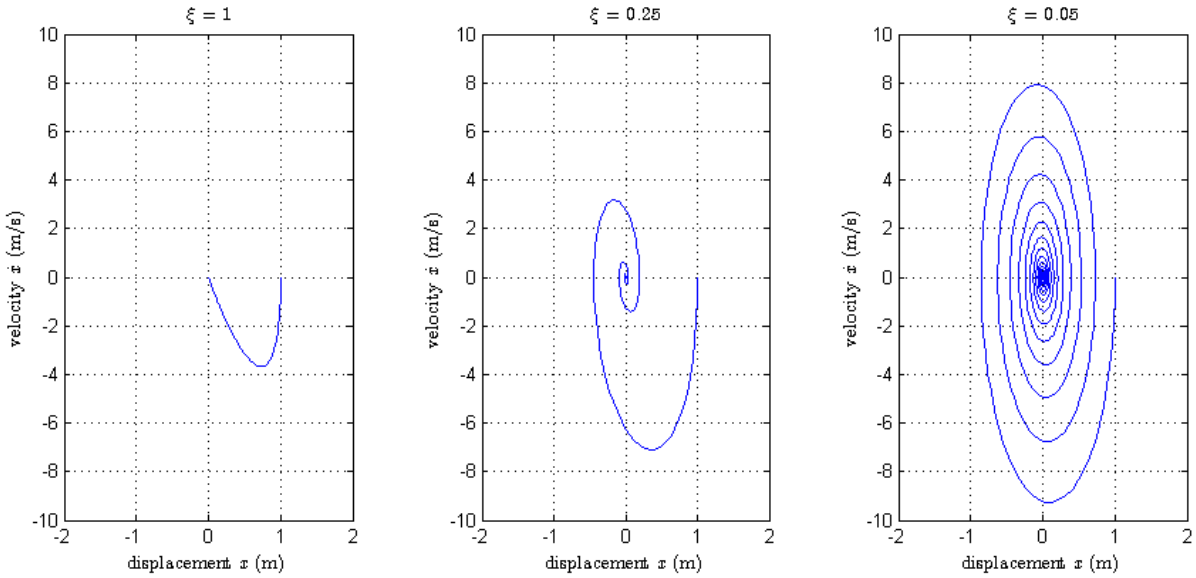

Figure 3.4: State planes for linear system for different damping ratios

For stability, we can apply the Floquent theory on the equation. For finding the transition curves we are going to use the Harmonic Balance Method, while more examples can be seen in (Dwivedy 2014) or (Ghandchi and Kalkowski 2016).

We expect the response to be as follows.

$$x(t) = A_1 \cdot cos(\frac{\omega_p t}{2}) + B_1 \cdot sin(\frac{\omega_p t}{2}) \tag{3.22}$$

We derive equation 3.22 and substitute it back into the 3.21. Then we separate the sines and cosines terms and we obtain:

$$\begin{bmatrix} \omega_n^2 + \omega_n^2 K_0 + \omega_n^2 \Delta K \frac{1}{2} - \frac{\omega_p^2}{4} & \xi\omega_n\omega_p \\ -\xi\omega_n\omega_p & \omega_n^2 + \omega_n^2 K_0 - \omega_n^2 \Delta K \frac{1}{2} - \frac{\omega_p^2}{4} \end{bmatrix} \begin{pmatrix} A_1 \\ B_1 \end{pmatrix} = \begin{pmatrix} 0 \\ 0 \end{pmatrix} \tag{3.23}$$

The determinant of this matrix have to be zero and all the coefficient have to be real. Then we can plot the transition curve for principal parametric resonance.

$$\Delta K = \frac{\sqrt{16(K_0+1)^2\omega_n^4 - 8\omega_n^2\omega_p^2(K_0 - 2\xi^2) + \omega_p^4}}{2\omega_n^2} \tag{3.24}$$

We can find principal parametric resonances on frequencies:

$$\omega_n^{Pr} = \frac{2\omega_n}{n} \tag{3.25}$$

Two tongues can be seen in Figure 3.5. The area above the transition curves is unstable while the area under is stable.

By partial derivation for ω_p, we are able to find the local minimum. Here is the equation for first Principle resonance. As you can see the stability depends on natural frequency, linear stiffness of the system and damping ratio.

$$\omega_1^{Pr} = 2\omega_n \cdot \sqrt{K_0 - 2\xi^2} \tag{3.26}$$

$$\Delta K_{krit}|_{\omega_p = \omega_1^{Pr}} = 4\xi \cdot \sqrt{K_0 - \xi^2} \tag{3.27}$$

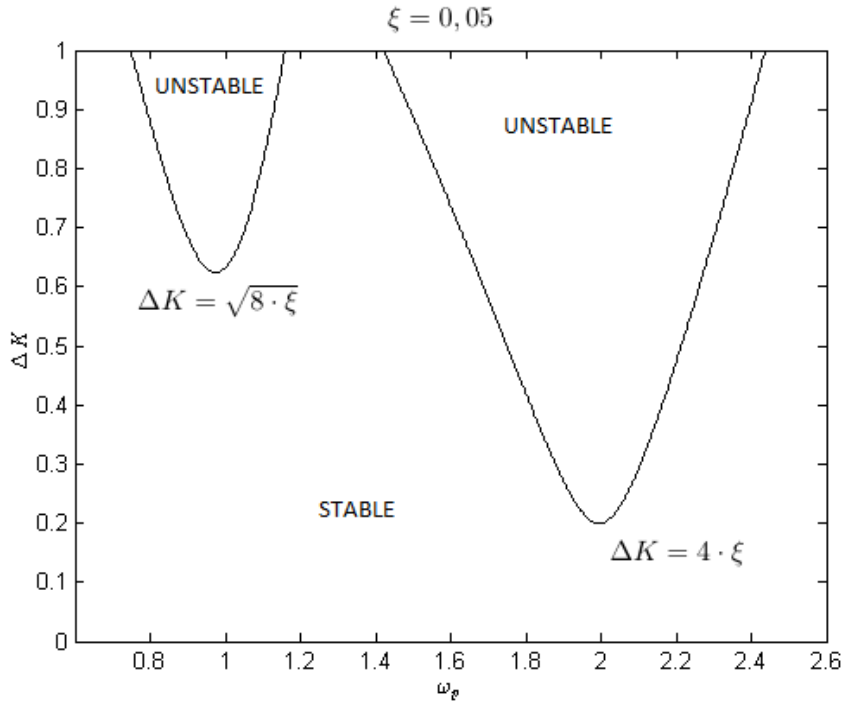

Figure 3.5: Stability regions of our system

You can see all the three states in Figure 3.6.

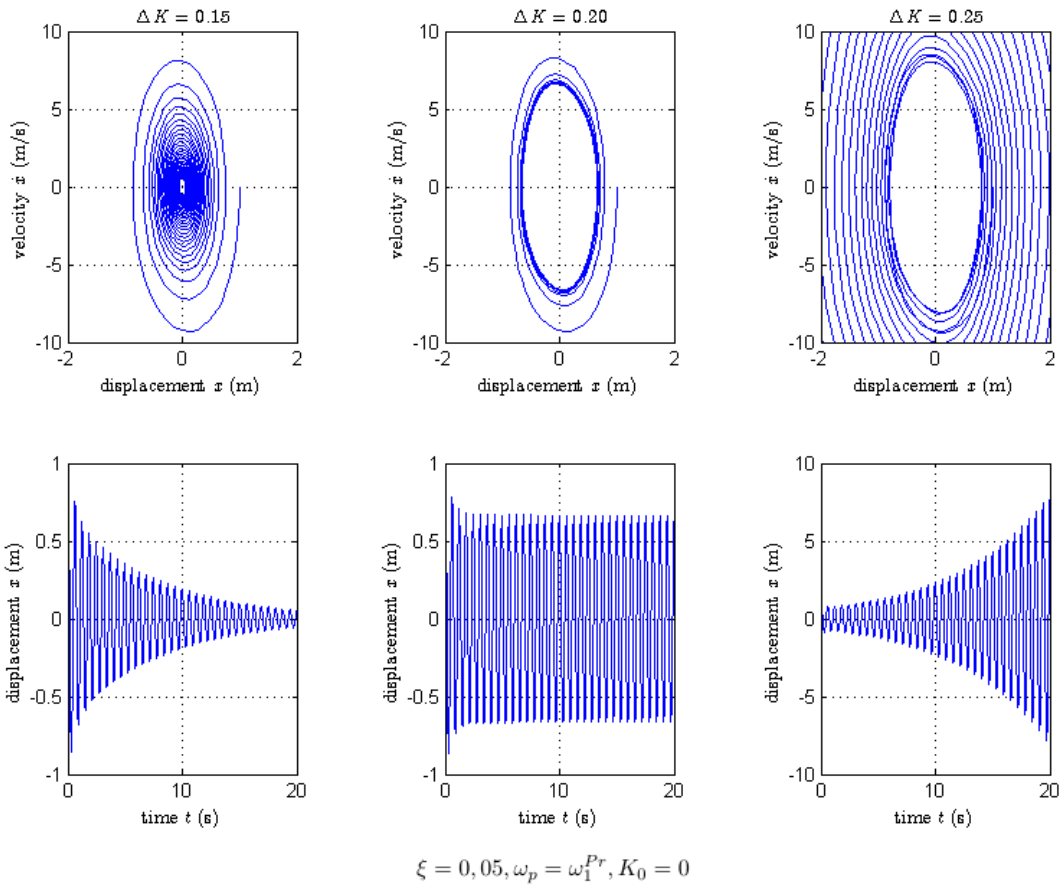

Figure 3.6: The stability states of Damped mathieu equation

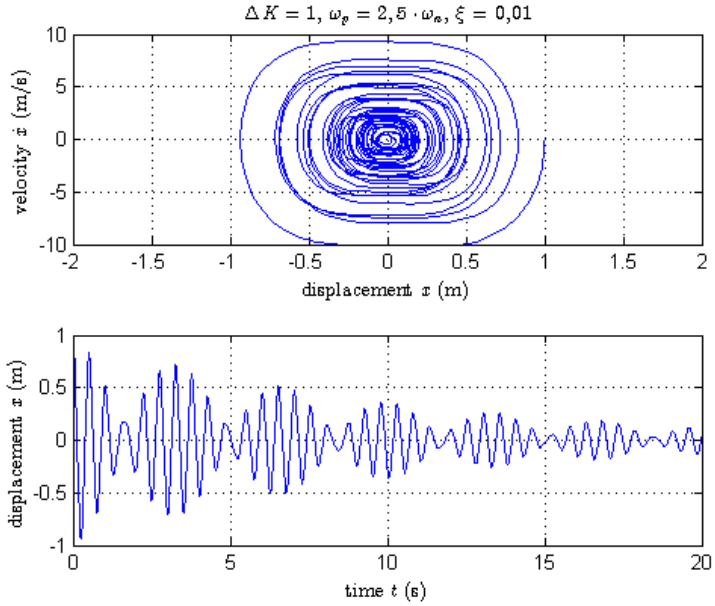

Figure 3.7: The equation behavior outside of parametric resonance

3.3 Simulation Model

Now we are going to create a simulation model from equations above. For these purposes, MATLAB Simulink program is used. Our complex problem is split into a few smaller parts. Basic control system from Figure 3.2 can be seen in Figure 3.8.

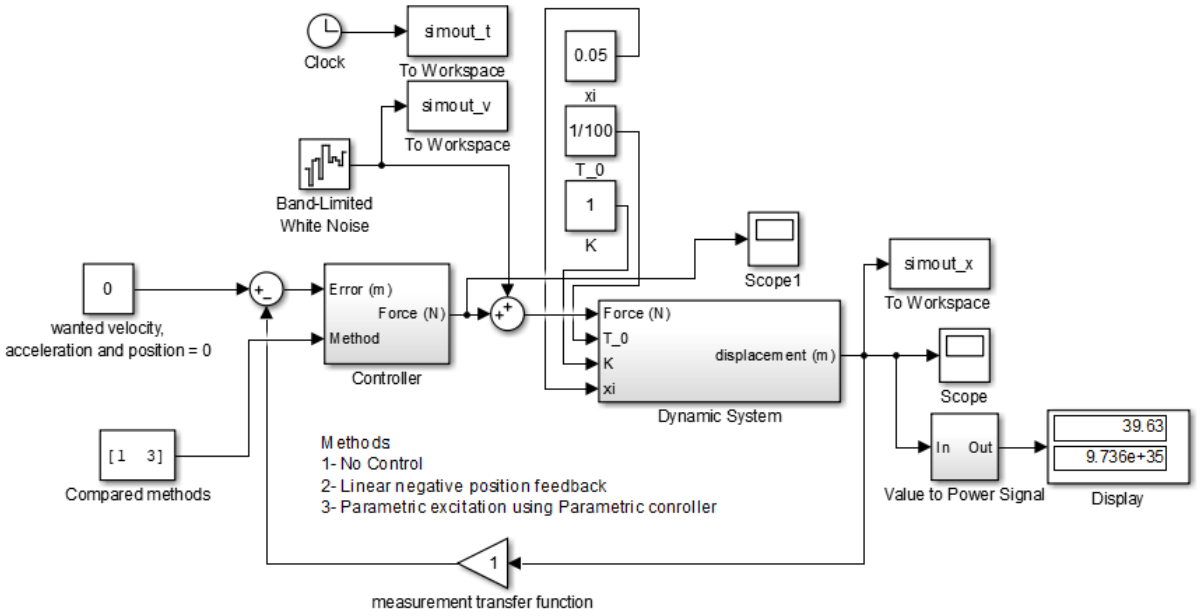

Figure 3.8: Basic control system simulation scheme

First, an important block is Dynamic System. Schema of this block can be seen in Figure 3.9. The transfer function of this system is:

$$G = \frac{1}{(\frac{1}{100})^2 s^2 + 2\xi \frac{1}{100} s + 1} \tag{3.28}$$

, where:

$$K = 1 \tag{3.29}$$

$$T_0 = \frac{1}{100} s \tag{3.30}$$

$$\xi = 0,05 \tag{3.31}$$

As a controller we can change between three modes- turn off, linear controller of the P-type and P-type controller with harmonic change.

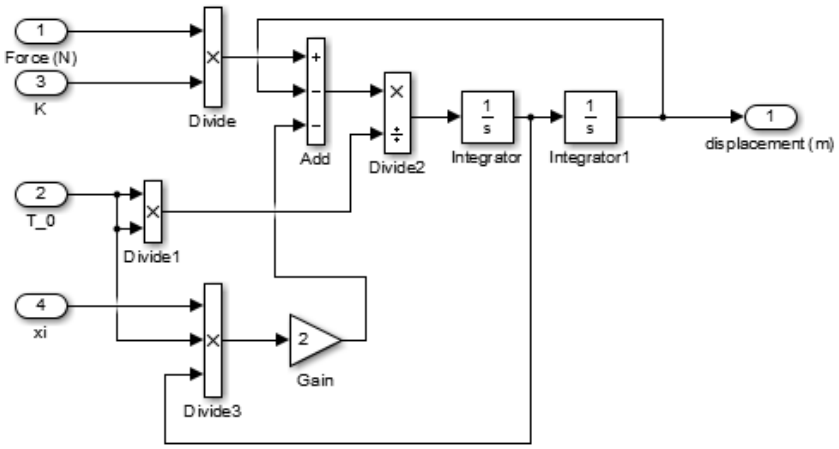

Figure 3.9: Simulation scheme of Second Order System

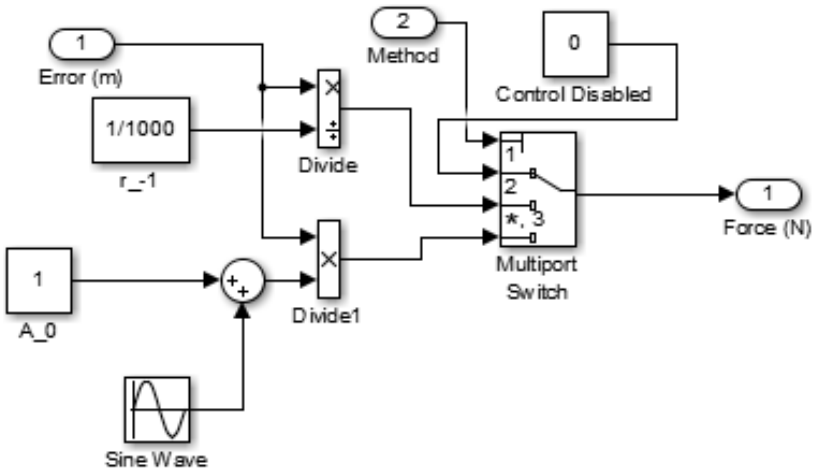

Figure 3.10: Simulation scheme of Controller

For future analyses of results, there is scope to show the results in the time domain, block "To Workspace" so we can make other post-simulation data analyses and block to calculate the power of signal so we can compare the effect of dumping. The content of that block can be seen in Figure 3.11. It can be described by equation 3.32.

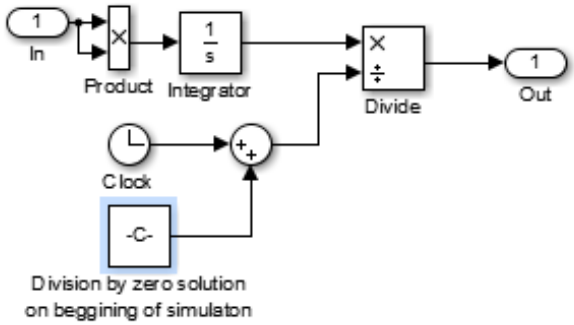

Figure 3.11: Simulation scheme of PW Block

$$PW = \frac{1}{t}\int x(t)^2 dt \tag{3.32}$$

```
% Parameters of the system
K = 1;
A_0 = 4;
xi = 0.05;
T_0 = 1/100;

% Local minimum calculation
K_0 = A_0 + K;
dKkrit = 4*xi*(K_0-xi^2).^(1/2)
dwkrit = 2*(1/T_0)*(K_0-2*xi^2).^(1/2)
```

Listing 3.1: Parametric stability local minimum calculation in Matlab

In figure 3.12 you can see the change in the PSD (Appendix A) of the system for different control approaches. After applying Negative Position Feedback we change the natural frequency of the system. If we then change the gain periodically on Principal Parametric Resonance the system is unstable and the magnitude of the system is much bigger then for resonance. In this picture, the parametric excitation is set to be in transition between stable and unstable area.

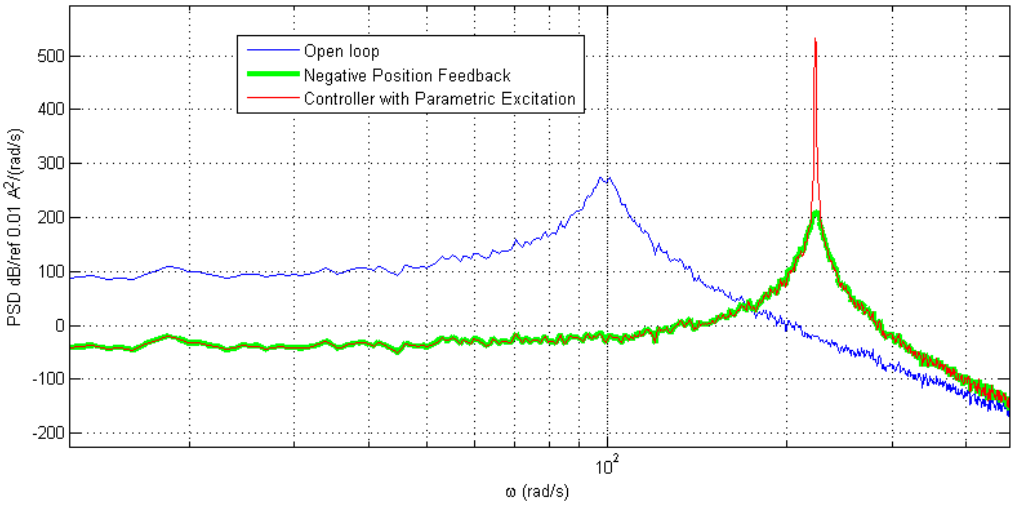

Figure 3.12: Power Spectral Density for our measurement (1DOF)

4 Multi Degree of Freedom Systems

4.1 Combination Parametric Resonances

The real oscillation systems usually contain more coupled modes of vibration. Because the system is not linear we can't use superposition. It is discovered (Tondl 2000) that near combination parametric resonance, the system is well damped.

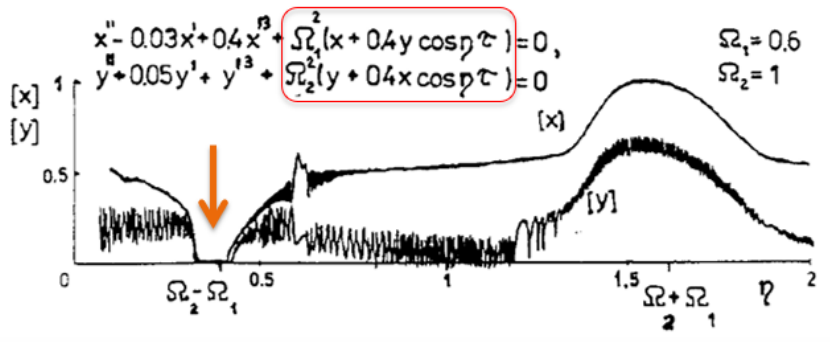

Figure 4.1: The damping of coupled systems (Tondl 2000)

In (Tůma et al. 2014a) was proved that this frequency has a positive effect on vibration damping by numerical simulation. The Combination Parametric Resonance frequencies can be calculated as (Tůma et al. 2014b):

$$\omega^{Cr}_{j\pm k,n} = \frac{\omega_j \pm \omega_k}{n} \tag{4.1}$$

, where ω_j and ω_k are natural frequencies of linear system. To describe more we are going to use very simple two mass system as shown in Figure 4.2.

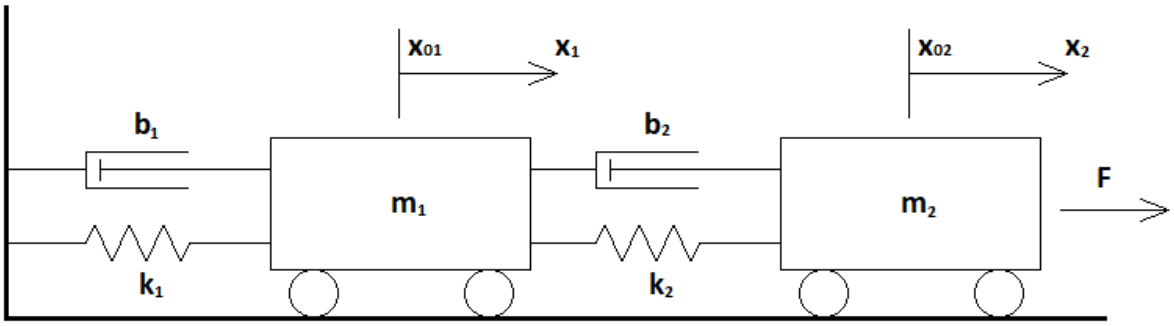

Figure 4.2: Simple Two Degree of Freedom coupled system

Differential equations of this system are:

$$m_1 \cdot \ddot{x}_1(t) = -k_1 \cdot x_1(t) - b_1 \cdot \dot{x}_1(t) + k_2 \cdot (x_2(t) - x_1(t)) + b_2 \cdot (\dot{x}_2(t) - \dot{x}_1(t)) \tag{4.2}$$

$$m_2 \cdot \ddot{x}_2(t) = F(t) - k_2 \cdot (x_2(t) - x_1(t)) - b_2 \cdot (\dot{x}_2(t) - \dot{x}_1(t)) \tag{4.3}$$

, where:
m_1 and m_2 are the bodies masses,
t is time variable,
$x_1(t)$ and $x_1(t)$ are the function of bodies displacement,
$F(t)$ is the function of the force acting on the body,
b_1 and b_2 are the dampens,
k_1 and k_2 are the stiffnesses of the system.

Since now we will use State-Space notation:

$$\dot{\mathbf{x}}(t) = \mathbf{A}\mathbf{x}(t) + \mathbf{B}\mathbf{u}(t) \tag{4.4}$$

$$\mathbf{y}(t) = \mathbf{c}^{\mathbf{T}}\mathbf{x}(t) + \mathbf{d}\mathbf{u}(t) \tag{4.5}$$

, where:
$\mathbf{x}(t)$ is called the "state vector",
$\mathbf{u}(t)$ is called the "input (or control) vector",
$\mathbf{y}(t)$ is called the "output vector",
$\mathbf{A}$ is the "state (or system) matrix",
$\mathbf{B}$ is the "input matrix",
$\mathbf{c}^{\mathbf{T}}$ is the "output matrix",
$\mathbf{d}$ is the "feedthrough (or feedforward) matrix".

After substitution:

$$\begin{bmatrix} \dot{x}_1(t) \\ \ddot{x}_1(t) \\ \dot{x}_2(t) \\ \ddot{x}_2(t) \end{bmatrix} = \begin{bmatrix} 0 & 1 & 0 & 0 \\ \frac{-k_1-k_2}{m_1} & & \frac{-b_1-b_2}{m_1} & & \frac{k_2}{m_1} & & \frac{b_2}{m_1} \\ 0 & 0 & 0 & 1 \\ \frac{k_2}{m_2} & & \frac{b_2}{m_2} & & \frac{-k_2}{m_2} & & \frac{-b_2}{m_2} \end{bmatrix} \begin{bmatrix} x_1(t) \\ \dot{x}_1(t) \\ x_2(t) \\ \dot{x}_2(t) \end{bmatrix} + \begin{bmatrix} 0 \\ 0 \\ 0 \\ \frac{1}{m_2} \end{bmatrix} \cdot F(t) \tag{4.6}$$

$$y(t) = \begin{bmatrix} 0 & 0 & 1 & 0 \end{bmatrix} \begin{bmatrix} x_1(t) \\ \dot{x}_1(t) \\ x_2(t) \\ \dot{x}_2(t) \end{bmatrix} + 0 \cdot \cdot F(t) \tag{4.7}$$

4.2 Simulation Model

Simulation Model is the same as our 1DoF model. The only change is that the dynamic system is different. Using Integrator blocks for more DoF systems is making the schema hard to understand. Other options are State-Space block or Transfer Function Block.

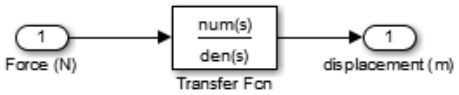

Figure 4.3: Dynamic system made by Transfer Function Block

Numerator and Denominator are calculated in Matlab.

```
% definition of variables
k1 = 10;
k2 = 10;
b1 = 0.01;
b2 = 0.01;
m1 = 0.05;
m2 = 0.01;

% filling the state-space matrices
A= [ 0 1 0 0 ; (-k1-k2)/m1 (-b1-b2)/m1 k2/m1 b2/m1 ; 0 0 0 1 ; k2/m2 b2/m2 -k2/
    m2 -b2/m2 ];
B= [0;0;0;1/m2];
C= [0 0 1 0];
D= 0;

% state-space to transfer function
[num,den] = ss2tf(A,B,C,D);

% plotting
G = tf(num,den)
```

```
bode(G);
```

Listing 4.1: Conversion from State-Space to Transfer Function in Matlab

First for this system we are going to simulate unwanted (for dampening process) states. By plotting PSD spectrum (Appendix A) we will find natural frequencies of the system:

$$\omega_{n1} = 16,87 \text{ rad/s} \tag{4.8}$$

$$\omega_{n1} = 46,02 \text{ rad/s} \tag{4.9}$$

Which mean that Principle Parametric resonances can be found on frequencies:

$$\omega_1^{Pr} = 33,74 \text{ rad/s} \tag{4.10}$$

$$\omega_1^{Pr} = 92,04 \text{ rad/s} \tag{4.11}$$

Another resonance which amplifies the oscillation can be found on Positive Combination Frequency:

$$\omega_{2+1,1}^{Cr} = \frac{\omega_n 2 + \omega_1}{1} = 62,82 \text{ rad/s} \tag{4.12}$$

All these states are shown in 4.4. Notice that on Principle resonance the second mode is not affected. On Combination Resonance Frequency both modes are amplified.

However, our main motivation is on frequency:

$$\omega_{2-1,1}^{Cr} = \frac{\omega_n 2 - \omega_1}{1} = 29,15 \text{ rad/s} \tag{4.13}$$

Exciting on this frequency has a positive effect on vibration damping as shown in Figure 4.5. Important is to remind that these frequencies are not dissipated but transported into other frequencies as shown in Figure 4.6.

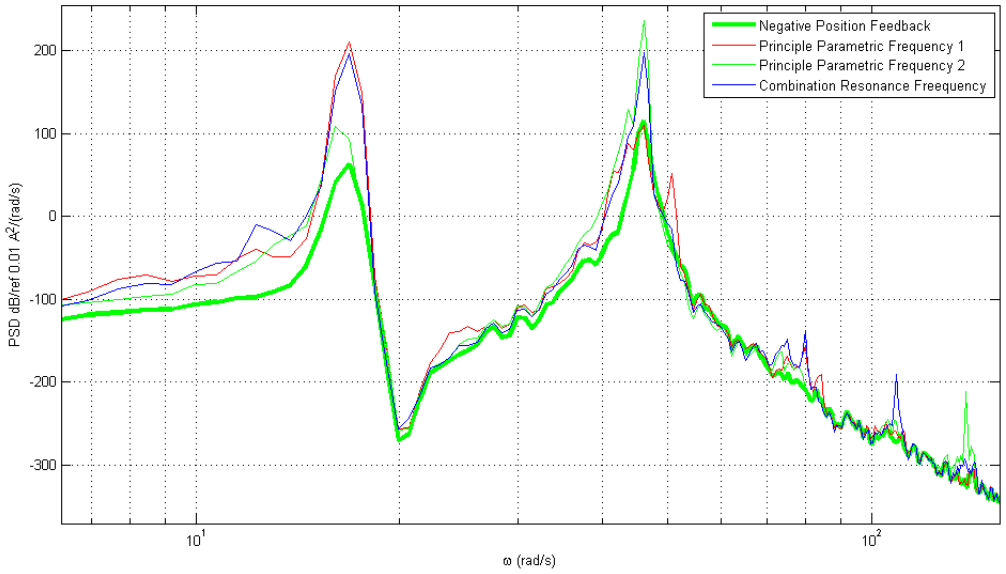

Figure 4.4: PSD of 2DoF system for our measurements (resonances)

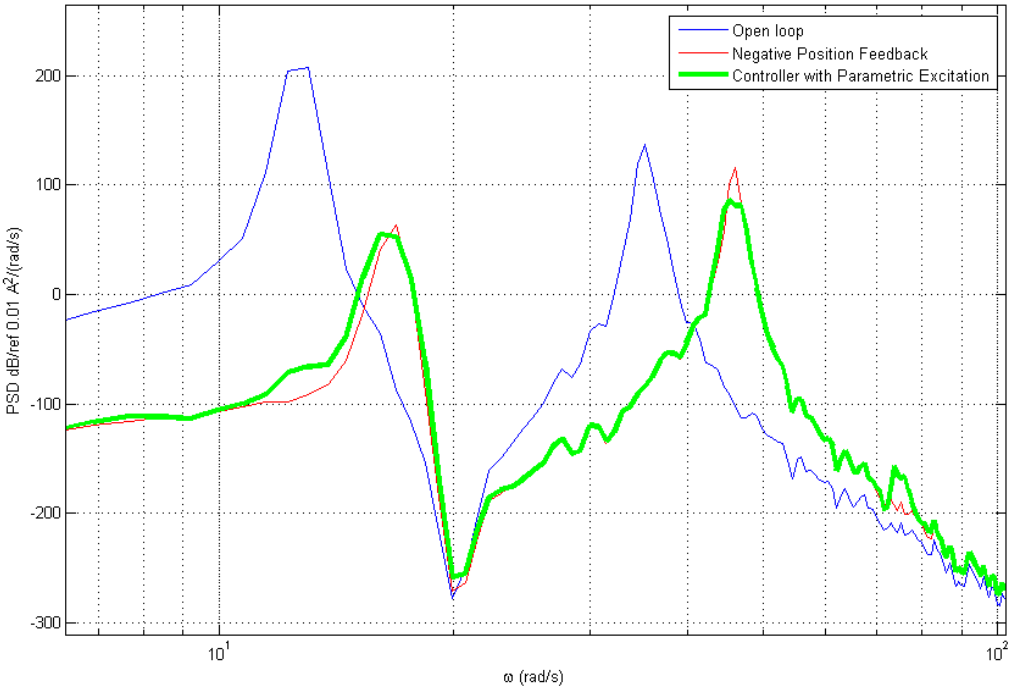

Figure 4.5: PSD of 2DoF system for our measurements (controlling)

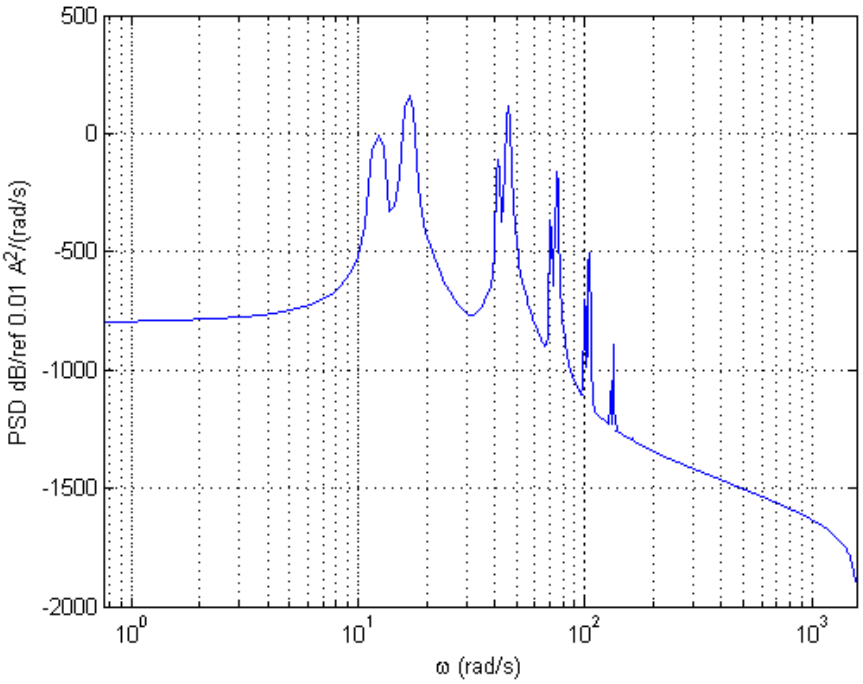

Figure 4.6: PSD of 2DoF system for our measurements (Sinusoidal input)

5 Practical application on the test rig

5.1 Test rig introduction

In this thesis, the experiment is made also using the cantilever beam which is a great example of the harmonic system. The purpose of using this method is not to enchant the step response but dampen the noise which influences every real system. A physical model can be seen in Figure 5.1. PPA-4022 and PPA 1001 (MIDÉ 2016) have been clamped to 1 mm thick aluminum beam. The beam is clamped to a vibrator (kinematic excitation) LDS V 400. The displacement is measured by Doppler laser. All inputs and outputs are connected with dSpace Control Board DS1104 (outputs through the amplifier). All inputs are then generated in HIL (Hardware in the Loop) system dSpace with use Simulink for controlling. The model is described with more details in (Štramberský 2016).

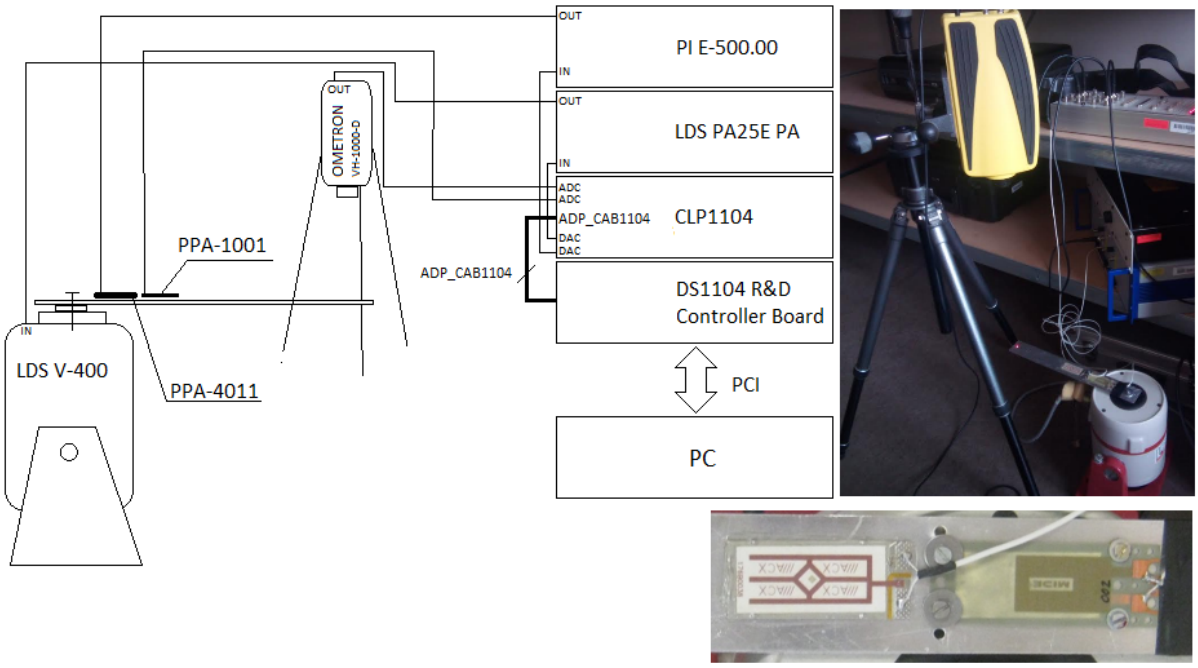

Figure 5.1: The physical model of the system

The dSpace is based on code generating from MATLAB Simulink. The advantage of this approach is that the same schemes that are used for real-time control can be used for simulation also. Therefore all the algorithm are made with that way that they work in real time. That is especially useful for Fourier analysis because the parametric excitation is not easily visible in time.

For control, the piezoelectric patch PPA-1001 output or laser can be used in feedback signal while the laser is used for plotting the output. The advantage of the doppler laser is that sensitivity is known and is not affected by clamping position and stiffness of beam-like piezoelectric sensors are. Interface for measuring is created in dSpace Control Desk 6.3 (Figure 5.2).

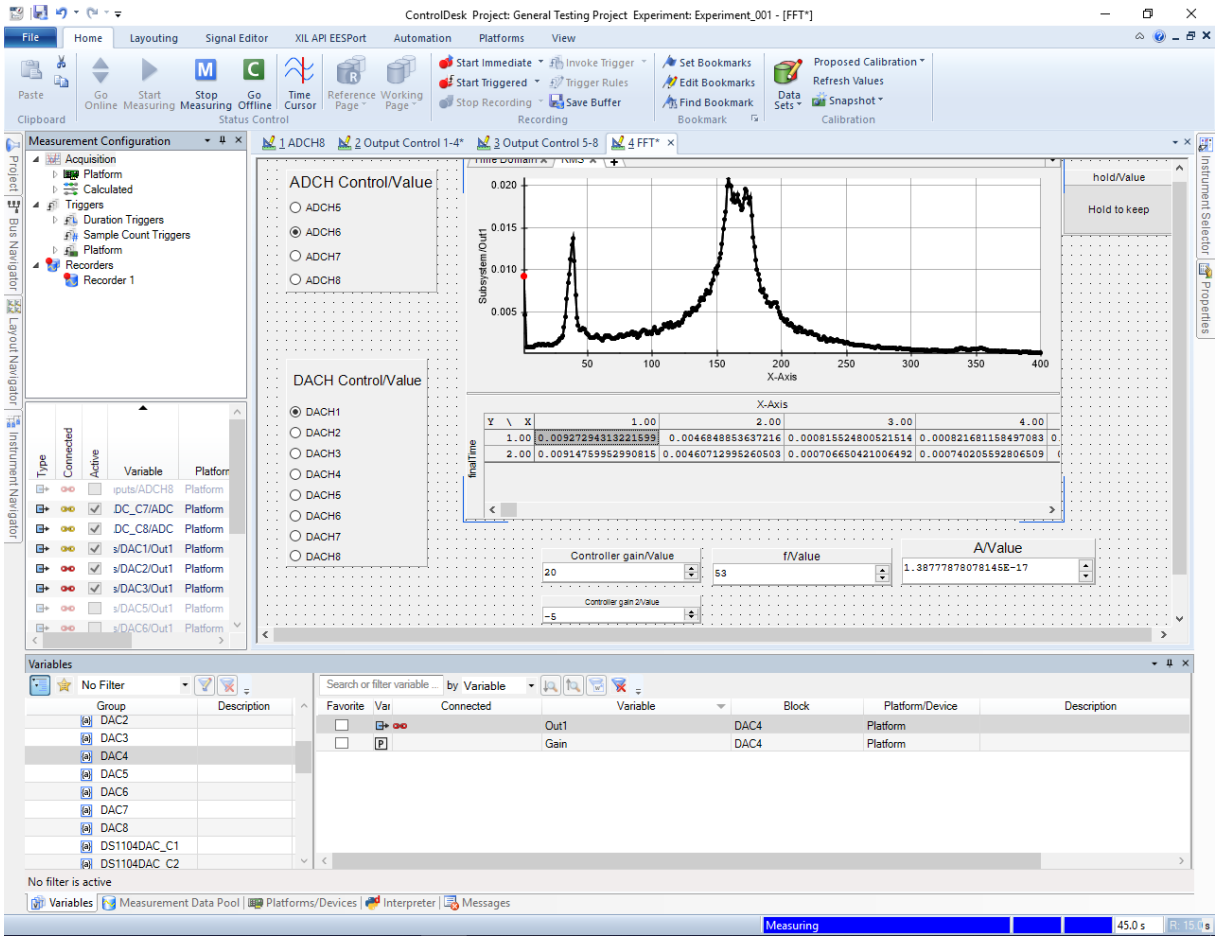

Figure 5.2: Graphic interface for measurements in dSpace ControlDesk 6.3

Important knowledge which should be mentioned is the nodes and modes. Cantilever beam contains an infinite amount of modes where the number of nodes is equal to the mode count. Therefore for non-collocated control (sensor and actuator are not on the same place), every second mode phase shift is 180 degree. That is important to remember because, for non-collocated control, negative feedback destabilizes even modes. Shapes of modes can be seen on picture 5.3.

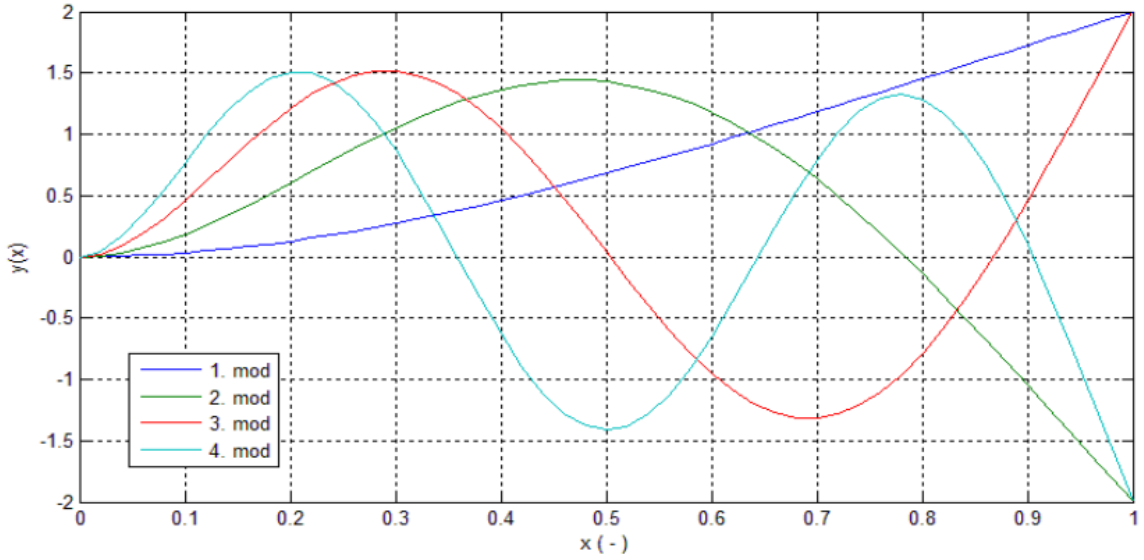

Figure 5.3: Modes and nodes of cantilever beam (Štramberský 2016)

5.2 Measuring data

As stated before, the control application is written in Matlab Simulink while visualization is made in dSpace Control Desk 6.3. The basic structure of the algorithm can be seen in Figure 5.4.

It contain subsystems:

- Inputs - Which take care of measuring connected inputs and normalize them.
- 8 blocks for our custom algorithms - Every block has 4 inputs connected to it and one output which can be influenced by these inputs.
- Outputs - This block contains setting as an output enable, output gain, limiters, rate limiters or output offset.
- Transfer function generator - This block is for generating TF functions or RMS spectrum.

For measuring the characteristic simple white noise generator is used which can be seen in 5.5. It is important to make sure that the noise is only strong enough to stay in the output limits of -1V to 1V.

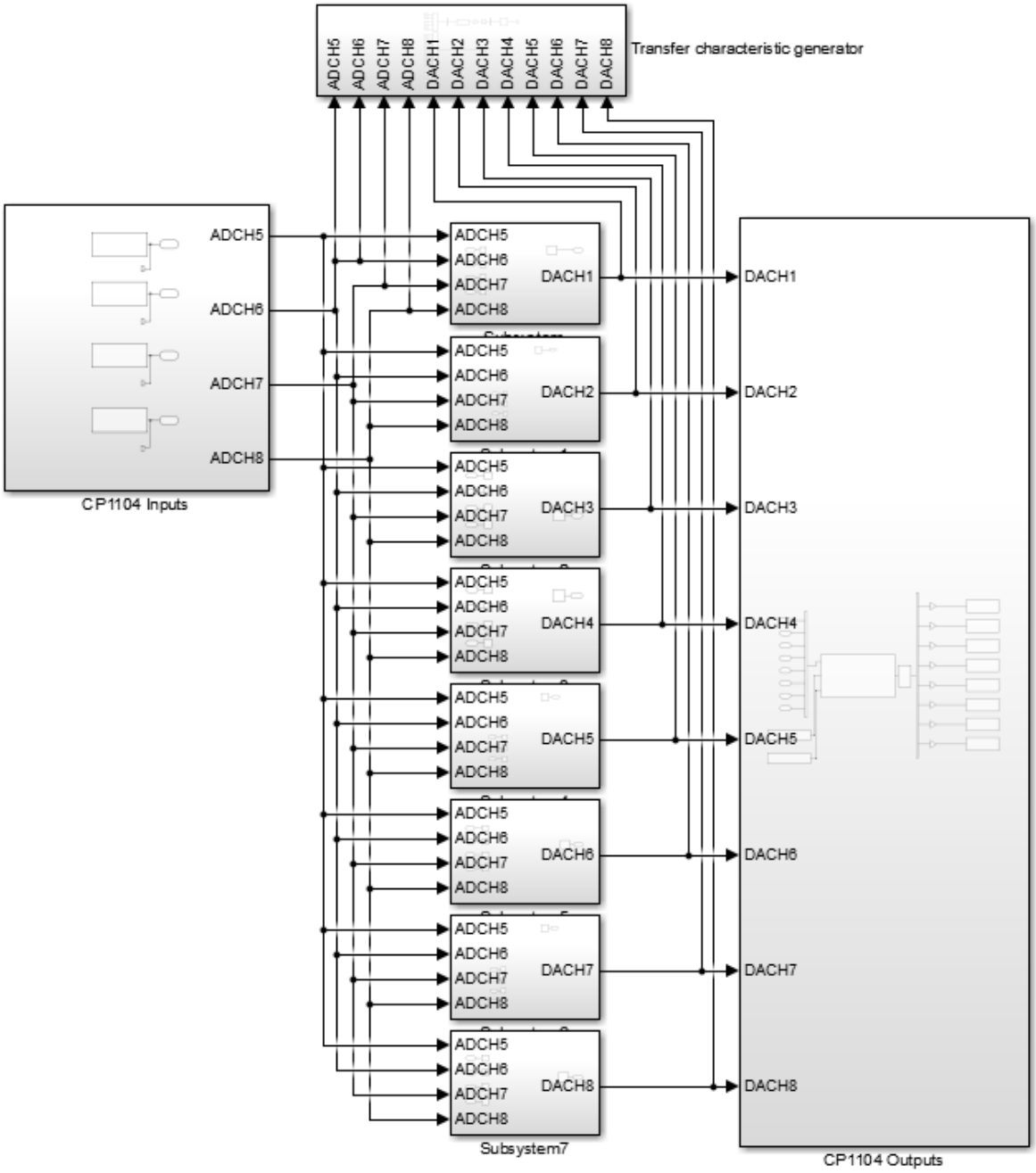

Figure 5.4: Basic structure of the algorithm loop

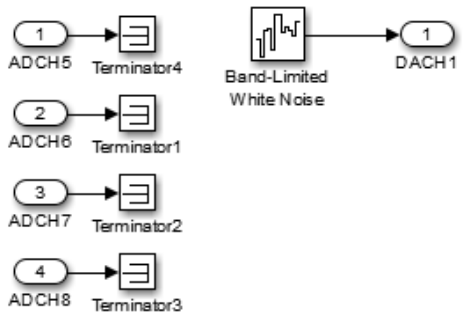

Figure 5.5: Simple white noise generator

Our piezo actuator limiting us by our amplifier which has output voltage range only between -20V and 120V. Also while the range of dSpace 1104 card is -10V to $+10$V, it is controlled by output with range -1V to 1V. Therefor for exciting piezoelectric actuator the offset is used to get as much as possible power from them. Updated scheme can be seen in Figure 5.6.

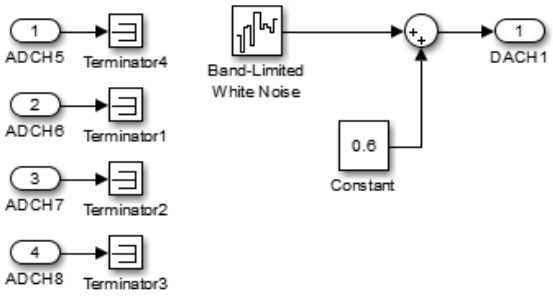

Figure 5.6: White noise generator for piezoelectric actuator limited by amplifier

Algorithm for measuring RMS spectrum (more about this method can be found in **??**) is made by these parts:

- Lowpass filter - Finite Element Filter (FIR) is used to remove frequencies higher than Nyquist Frequency to prevent aliasing.
- Saving to buffer - For Fourier transform (FFT) we need N points.
- Multiplication by time window - To make the measurement more accurate, because of the discrete error we choose hamming window.
- Transformation from the time domain to the frequency domain using FFT.
- Absolute value - For RMS we are not interested in phase.
- Multiplication by $\frac{2}{N \cdot \sqrt{2}}$ to get RMS value.

- Halving the spectrum, because the second half is the mirror of the first half.
- Averaging the results to make them more accurate. Overlapping $\frac{2}{3}$ is used which is recommended for Hamming window. (Tůma 2014)

The scheme of this can be seen in Figure 5.7.

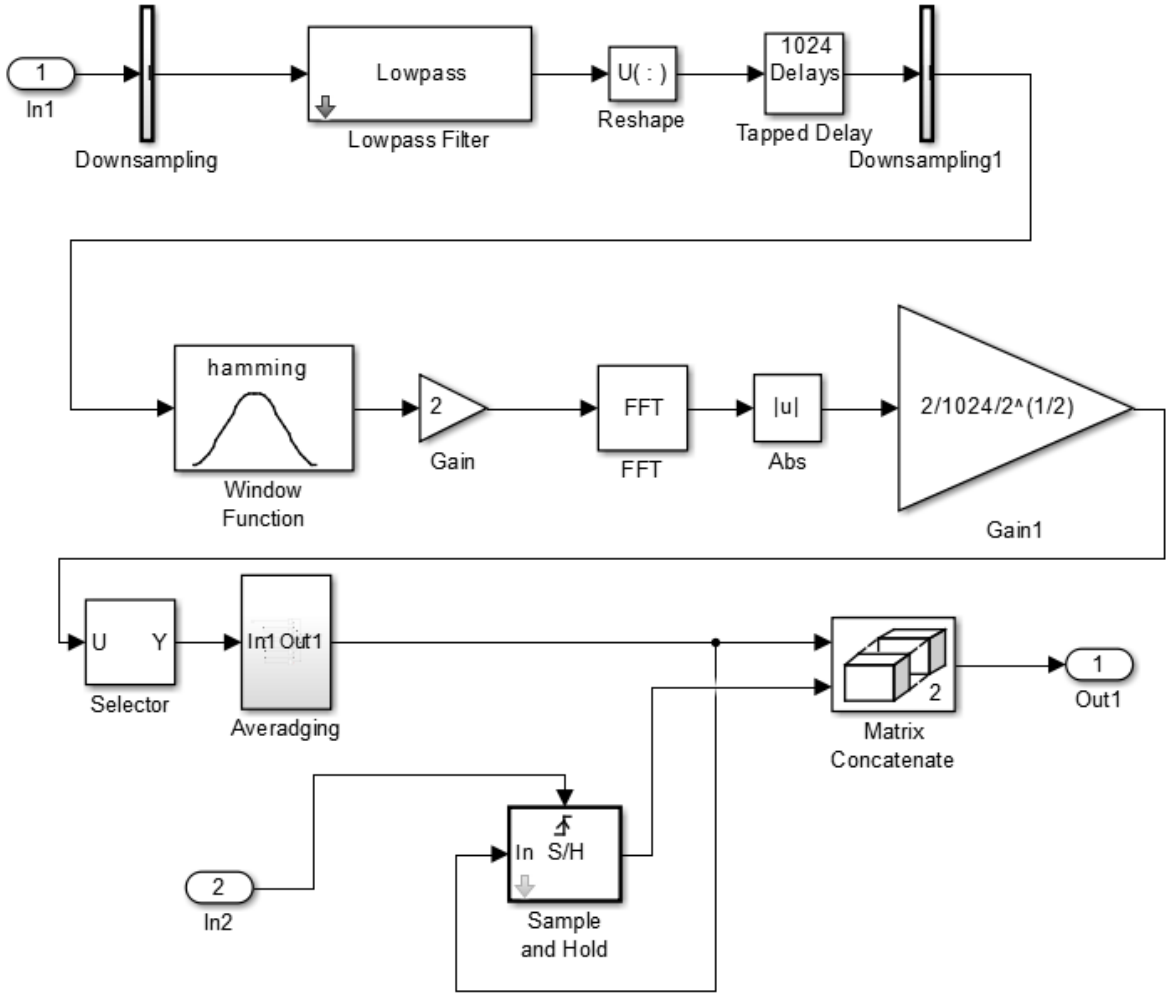

Figure 5.7: RMS spectrum generator made in Simulink

Another important part of measurements is by creating frequency characteristics. The same method as for RMS spectrum generation is used (Harmonic analysis). Only a few differences have to be considered to create the frequency characteristic:

- Both, the input and the output, is need to be measured at the same time. Then we create the transformation for both signals.

- Because both of our sensors measure velocity, we need to integrate (high sampling frequency) to receive the displacement and use lowpass filter.
- Instead of calculating the absolute value of FFT images we take the whole complex number and receive the frequency characteristic by equations:

$$A(n) = 20 \cdot \log \frac{Y(n)Y^*(n)}{X(n)Y^*(n)} \tag{5.1}$$

$$\phi(n) = \arg \frac{Y(n)Y^*(n)}{X(n)Y^*(n)} \tag{5.2}$$

, where n is the index of FFT image,
$Y(n)$ is output FFT image,
$X(n)$ is input FFT image,
and * is complex conjugate of the images.

To give to the indexes meaning we make the transformation to frequency:

$$f_{max} = \frac{1}{T_s \cdot 2} \tag{5.3}$$

$$f(n) = \frac{f_{max} \cdot n}{N_{FFT}} \tag{5.4}$$

where f_{max} is the maximal measured frequency,
T_s is sampling period,
N_{FFT} is the number of samples use for the FFT transformation.

The Simulink scheme can be seen in Figure 5.8.

Used dSpace is capable of measuring with sampling period up to $T_s = 0,001$s. Here there is used downsampling to sampling period $T_s = 0,003$s, which mean that we can measure frequencies up to:

$$f_{max} = \frac{1}{T_s \cdot 2} = \frac{1}{0,003 \cdot 2} = 166,66\text{Hz} \tag{5.5}$$

, which is enough for us, because we want investigate first two modes which are in 100 Hz mark. For FFT transformation, 1024 samples is used. Because we use overlapping $\frac{2}{3}$, we down-sampling

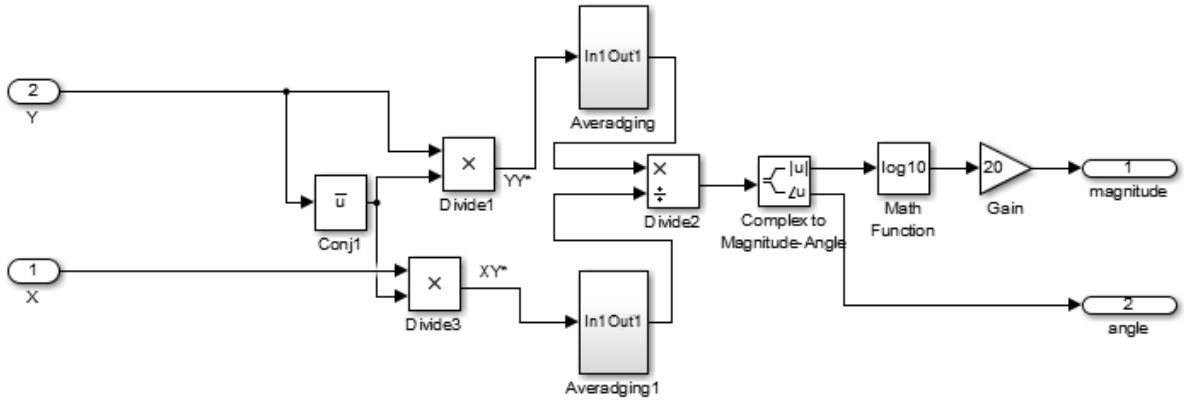

Figure 5.8: Calculating the frequency characteristics

the FFT to:

$$T_{FFT} = T_s \cdot N_{FFT} \cdot (1 - overlapping) = 0,003 \cdot 1024 \cdot (1 - \frac{2}{3}) = 1,024\text{s} \tag{5.6}$$

The Simulink code generator is capable of running on different frequencies if we use the "treat as an atomic unit" setting and set the sample rate. These blocks are called "Downsampling" in schemes.

5.3 Model of the test rig approximation

To create a model of the cantilever beam test rig different systems are commonly used and different methods of approximations can be used. This is well described in (Døssing 1989). In this thesis, the model based on frequency characteristic with multiple DoF is used. We investigate the first two modes of vibrations. The final transfer function is:

$$G(s) = (\frac{k_1 s}{T_1^2 s^2 + 2T_1\xi_1 s + 1} - \frac{k_2 s}{T_2^2 s^2 + 2T_2\xi_2 s + 1}) \cdot \frac{k_m}{T_m s + 1} \cdot \frac{1}{s} \tag{5.7}$$

where $\frac{1}{s}$ is transformation from velocity to position.

The Doppler Laser's parameters are:

$$k_m = 0.001 \frac{\text{V}}{\text{mm} \cdot \text{s}^{-1}} \tag{5.8}$$

$$T_m \approx 1\text{ms} \tag{5.9}$$

To make are approximation simpler, we make an assumption that:

$$k_m = \frac{0,5}{500} \frac{\text{V}}{\text{mm/s} \cdot \text{s}^{-1}} \tag{5.10}$$

$$T_m = 0\text{ms} \tag{5.11}$$

, so these values will appear inside T_1,T_2. Also inputs and outputs are normalized in range -1 to 1 V.

There are many methods of frequency characteristic approximation described in (Døssing 1989) like finding a Residuum. Because we choose to create our Model in real time, we choose a Gradient Descent algorithm which is the popular Machine Learning iteration algorithm.

Gradient Descent is often used for functions approximation. It works by gradually optimizing the parameter by calculating the partial derivation of the MSE (Mean Squared Error) which give as the slope of error so we know if the parameter should be increased or decreased. Very popular methods are using ARX or similar models and use the least square optimization. I personally believed that Gradient Descent method is more clear to understanding and change gradually which is useful for real-time application.

MSE can be calculated as:

$$MSE(k_1, T_1, \xi_1, k_2, T_2, \xi_2, i) = \frac{1}{n} \cdot \sum_{i=1}^{n} (f(k_1, T_1, \xi_1, k_2, T_2, \xi_2, i) - y(i))^2 \tag{5.12}$$

where i is the index of the point of discrete approximation,
$f(k_1, T_1, \xi_1, k_2, T_2, \xi_2, i)$ is the chosen function of approximated model,
and $y(i)$ is measured value.

Because we know our system well enough, we can approximate only Amplitude frequency characteristic. For Doppler laser, the change of phase (180 deg) is known. Amplitude charac-

teristic function can be calculated as:

$$f(k_1, T_1, \xi_1, k_2, T_2, \xi_2, i) = |G_1(\omega(i)j) - G_2(\omega(i)j)| = \\ = \omega(i) \cdot \sqrt{(a(k_1, T_1, \xi_1, i) - b(k_2, T_2, \xi_2, i))^2 + (c(k_2, T_2, \xi_2, i) - d(k_1, T_1, \xi_1, i))^2} \tag{5.13}$$

, where

$$a(k_1, T_1, \xi_1, i) = \frac{k_1(1 - T_1^2\omega^2(i)}{4T_1^2\omega^2(i)\xi_1^2 + (1 - T_1^2\omega^2(i))^2} \tag{5.14}$$

$$b(k_2, T_2, \xi_2, i) = \frac{k_2(1 - T_2^2\omega^2(i)}{4T_2^2\omega^2(i)\xi_2^2 + (1 - T_2^2\omega^2(i))^2} \tag{5.15}$$

$$c(k_2, T_2, \xi_2, i) = \frac{2T_2k_2\omega(i)\xi_2}{4T_2^2\omega^2(i)\xi_2^2 + (1 - T_2^2\omega^2(i))^2} \tag{5.16}$$

$$d(k_1, T_1, \xi_1, i) = \frac{2T_1k_1\omega(i)\xi_1}{4T_1^2\omega^2(i)\xi_1^2 + (1 - T_1^2\omega^2(i))^2} \tag{5.17}$$

With that, we are able to calculate MSE. For partial derivation we need to make a few simplifications:

$$\frac{\partial MSE(\theta, i)}{\partial \theta} = \frac{1}{n} \cdot \sum_{i=1}^{n} \frac{\partial}{\partial \theta}(f(\theta, i) - y(i))^2 = 2(f(\theta, i) - y(i))\frac{\partial f(\theta, i)}{\partial \theta} \tag{5.18}$$

, where θ is the vector of parameters k_1, T_1, ξ_1, k_2, T_2 and ξ_2.

$$\frac{\partial f(\theta_1, \theta_2, i)}{\partial \theta_1} = \omega^2(i) \cdot \sqrt{(a(\theta_1, i) - b(\theta_2, i))^2 + (c(\theta_2, i) - d(\theta_1, i))^2} = \\ = \omega^2(i) \cdot \frac{\frac{\partial a(\theta_1, i)}{\partial \theta_1}(a(\theta_1, i) - b(\theta_2, i)) - \frac{\partial d(\theta_1, i)}{\partial \theta_1}(c(\theta_2, i) - d(\theta_1, i))}{f(\theta_1, \theta_2, i)} \tag{5.19}$$

$$\frac{\partial f(\theta_1, \theta_2, i)}{\partial \theta_2} = \omega^2(i) \cdot \sqrt{(a(\theta_1, i) - b(\theta_2, i))^2 + (c(\theta_2, i) - d(\theta_1, i))^2} = \\ = \omega^2(i) \cdot \frac{\frac{\partial c(\theta_2, i)}{\partial \theta_2}(c(\theta_2, i) - d(\theta_1, i)) - \frac{\partial b(\theta_2, i)}{\partial \theta_2}(a(\theta_1, i) - b(\theta_2, i))}{f(\theta_1, \theta_2, i)} \tag{5.20}$$

, where θ_1 is the vector of parameters k_1, T_1, ξ_1
and θ_2 is the vector of parameters k_2, T_2 and ξ_2.

While all of these calculations are common for all parameters, every parameter has its own two partial derivations giving us a total of 12 equations:

$$\frac{\partial a(k_1, T_1, \xi_1, i)}{\partial k_1} = \frac{1 - T_1^2\omega^2(i)}{4T_1^2\omega^2(i)\xi_1^2 + (1 - T_1^2\omega^2(i))^2} \tag{5.21}$$

$$\frac{\partial d(k_1, T_1, \xi_1, i)}{\partial k_1} = \frac{4T_1^2\omega^2(i)\xi_1^2}{4T_1^2\omega^2(i)\xi_1^2 + (1 - T_1^2\omega^2(i))^2} \tag{5.22}$$

$$\frac{\partial a(k_1, T_1, \xi_1, i)}{\partial T_1} = \frac{2k_1T_1\omega^2(i)(T_1^4\omega^4(i) - 2T_1^2\omega^2(i) - 4\xi_1^2 + 1)}{(T_1^4\omega^4(i) + 2T_1^2\omega^2(i)(2\xi_1^2 - 1) + 1)^2} \tag{5.23}$$

$$\frac{\partial d(k_1, T_1, \xi_1, i)}{\partial T_1} = -\frac{2k_1\omega(i)\xi_1(3T^4\omega^4(i) + 2T_1^2\omega^2(i)(2\xi_1^2 - 1) - 1)}{(T_1^4\omega^4(i) + 2T_1^2\omega^2(i)(2\xi_1^2 - 1) + 1)^2} \tag{5.24}$$

$$\frac{\partial a(k_1, T_1, \xi_1, i)}{\partial \xi_1} = \frac{8k_1T_1^2\omega^2(i)\xi_1(1 - T_1^2\omega^2(i))}{(T_1^4\omega^4(i) + 2T_1^2\omega^2(i)(2\xi_1^2 - 1) + 1)^2} \tag{5.25}$$

$$\frac{\partial d(k_1, T_1, \xi_1, i)}{\partial \xi_1} = \frac{2k_1(T_1^5\omega^5(i) - 2T_1^3\omega^3(i)(2\xi_1^2 + 1) + T_1\omega(i))}{(T_1^4\omega^4(i) + 2T_1^2\omega^2(i)(2\xi_1^2 - 1) + 1)^2} \tag{5.26}$$

$$\frac{\partial b(k_2, T_2, \xi_2, i)}{\partial k_2} = \frac{1 - T_2^2\omega^2(i)}{4T_2^2\omega^2(i)\xi_2^2 + (1 - T_2^2\omega^2(i))^2} \tag{5.27}$$

$$\frac{\partial c(k_2, T_2, \xi_2, i)}{\partial k_2} = \frac{2T_2\omega(i)\xi_2}{4T_2^2\omega^2(i)\xi_2^2 + (1 - T_2^2\omega^2(i))^2} \tag{5.28}$$

$$\frac{\partial b(k_2, T_2, \xi_2, i)}{\partial T_2} = \frac{2k_2T_2\omega^2(i)(T_2^4\omega^4(i) - 2T_2^2\omega^2(i) - 4\xi_2^2 + 1)}{(T_2^4\omega^4(i) + 2T_2^2\omega^2(i)(2\xi_2^2 - 1) + 1)^2} \tag{5.29}$$

$$\frac{\partial c(k_2, T_2, \xi_2, i)}{\partial T_2} = -\frac{4k_2\omega(i)\xi_2(3T_2^4\omega^4(i) + 2T_2^2\omega^2(i)(2\xi_2^2 - 1) - 1)}{(T_2^4\omega^4(i) + 2T_2^2\omega^2(i)(2\xi_2^2 - 1) + 1)^2} \tag{5.30}$$

$$\frac{\partial b(k_2, T_2, \xi_2, i)}{\partial \xi_2} = -\frac{8k_2T_2^2\omega^2(i)\xi_2(1 - T_2^2\omega^2(i))}{(T_2^4\omega^4(i) + 2T_2^2\omega^2(i)(2\xi_2^2 - 1) + 1)^2} \tag{5.31}$$

$$\frac{\partial c(k_2, T_2, \xi_2, i)}{\partial \xi_2} = \frac{2T_2k_2\omega(i)}{4T_2^2\omega^2(i)\xi_2^2 + (1 - T_2^2\omega^2(i))^2} - \frac{16T_2^3k_2\omega^3(i)\xi^2}{(4T_2^2\omega^2(i)\xi_2^2 + (1 - T_2^2\omega^2(i))^2)^2} \tag{5.32}$$

All these equations work for non-collocated setting which is usually used (excitation from the fixed end while measuring the free end).

For collocated setting the partial derivations stay the same but equations 5.7, 5.13, 5.19,

5.20 change to:

$$G(s) = \left(\frac{k_1 s}{T_1^2 s^2 + 2T_1\xi_1 s + 1} + \frac{k_2 s}{T_2^2 s^2 + 2T_2\xi_2 s + 1}\right) \cdot \frac{k_m}{T_m s + 1} \cdot \frac{1}{s} \tag{5.33}$$

$$\begin{aligned} f(k_1, T_1, \xi_1, k_2, T_2, \xi_2, i) = |G_1(\omega(i)j) + G_2(\omega(i)j)| = \\ = \omega(i) \cdot \sqrt{\left(a(k_1, T_1, \xi_1, i) + b(k_2, T_2, \xi_2, i)\right)^2 + \left(-c(k_2, T_2, \xi_2, i) - d(k_1, T_1, \xi_1, i)\right)^2} \end{aligned} \tag{5.34}$$

$$\frac{\partial f(\theta_1, \theta_2, i)}{\partial \theta_1} = \omega^2(i) \cdot \frac{\frac{\partial a(\theta_1, i)}{\partial \theta_1}(a(\theta_1, i) + b(\theta_2, i)) - \frac{\partial d(\theta_1, i)}{\partial \theta_1}(-c(\theta_2, i) - d(\theta_1, i))}{f(\theta_1, \theta_2, i)} \tag{5.35}$$

$$\frac{\partial f(\theta_1, \theta_2, i)}{\partial \theta_2} = \omega^2(i) \cdot \frac{-\frac{\partial c(\theta_2, i)}{\partial \theta_2}(-c(\theta_2, i) - d(\theta_1, i)) + \frac{\partial b(\theta_2, i)}{\partial \theta_2}(a(\theta_1, i) + b(\theta_2, i))}{f(\theta_1, \theta_2, i)} \tag{5.36}$$

Implementation can be seen in Figures 5.9 to 5.12. In every iteration, the slope is calculated and they multiplied by learning rate. Learning rate is good to be changing to save time and make the optimization more accurate and faster. To keep this thesis simple I am not going to describe this in this thesis.

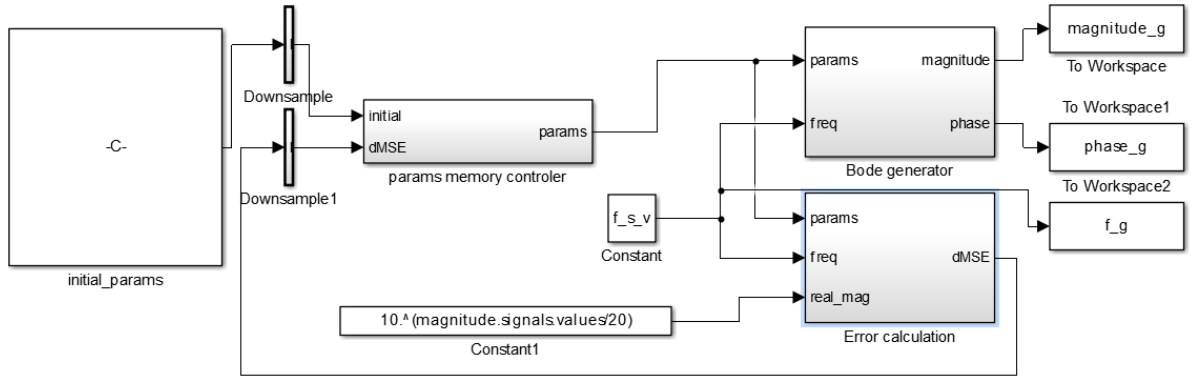

Figure 5.9: Frequency characteristic: basic control diagram

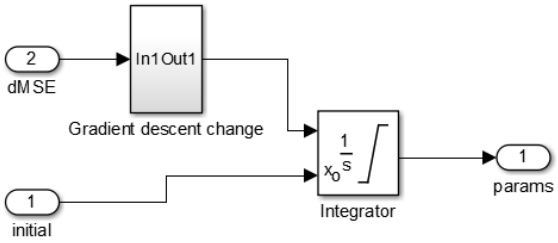

Figure 5.10: Gradient Descent algorithm: learning block

As seen in Table 5.1 and Figure 5.13 I made validation of algorithm by creating the demo

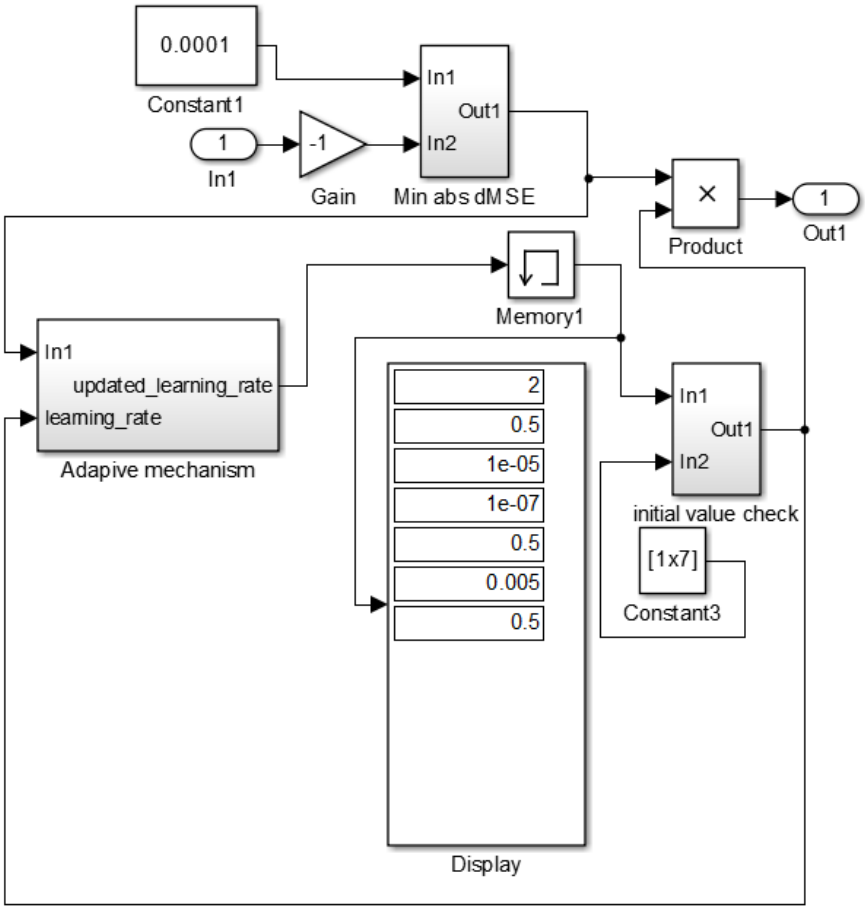

Figure 5.11: Gradient Descent algorithm: learning rates

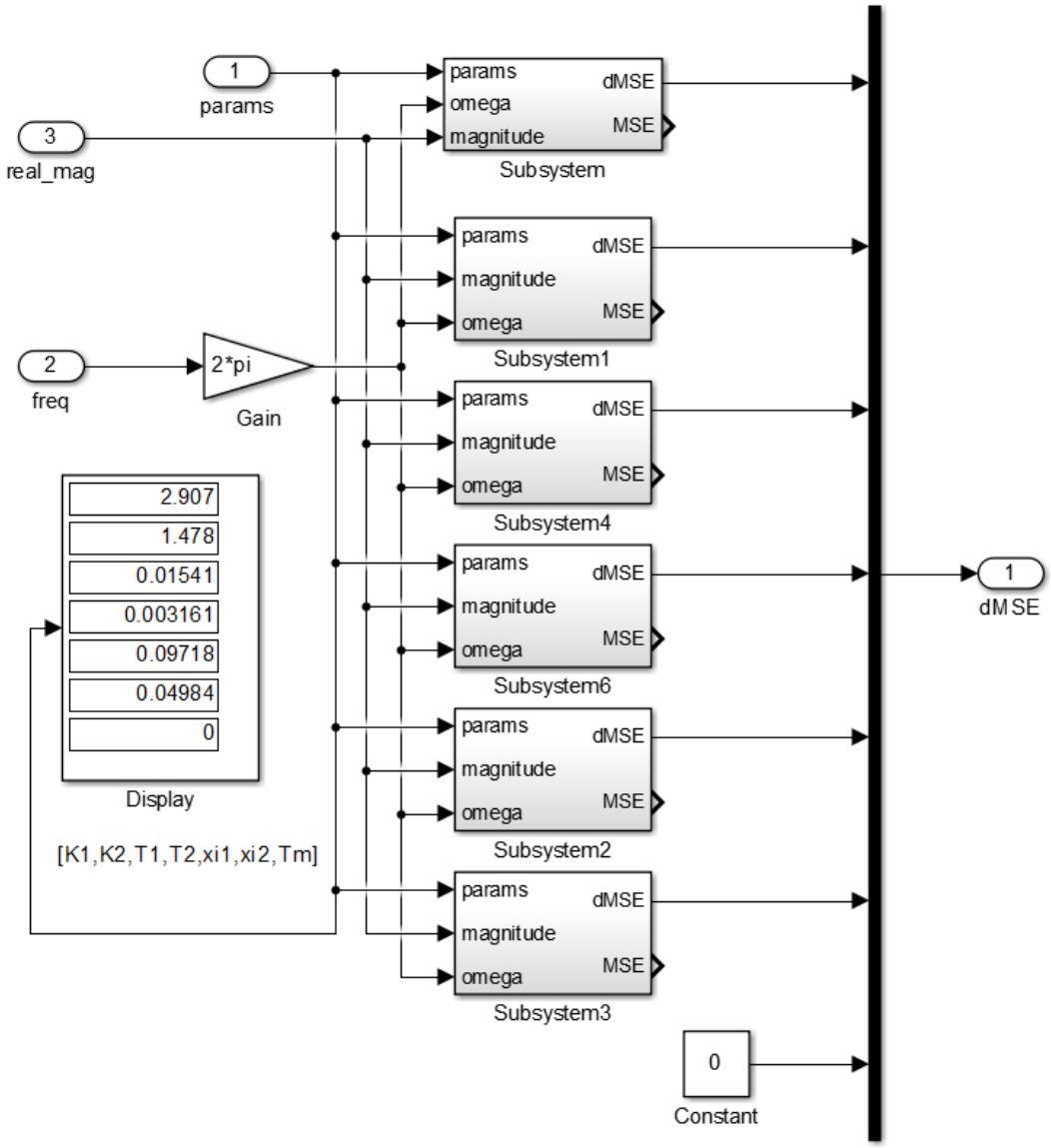

Figure 5.12: Gradient Descent algorithm: error calculating

model, exciting it with the white noise input signal, creating the FFT transformation and then using the Gradient Descent algorithm to make the approximation. We can see that quality is accurate enough. No comparison with another method has been made.

Table 5.1: Quality of Gradient Descent Approximation

Parameter	Original	Estimated
k_1	3	2.907
T_1	$\frac{1}{2\pi 10}$	$\frac{1}{2\pi 10{,}328}$
ξ_1	0,1	0,097
k_2	1,5	1,478
T_2	$\frac{1}{2\pi 50}$	$\frac{1}{2\pi 50.35}$
ξ_2	0.05	0,00498

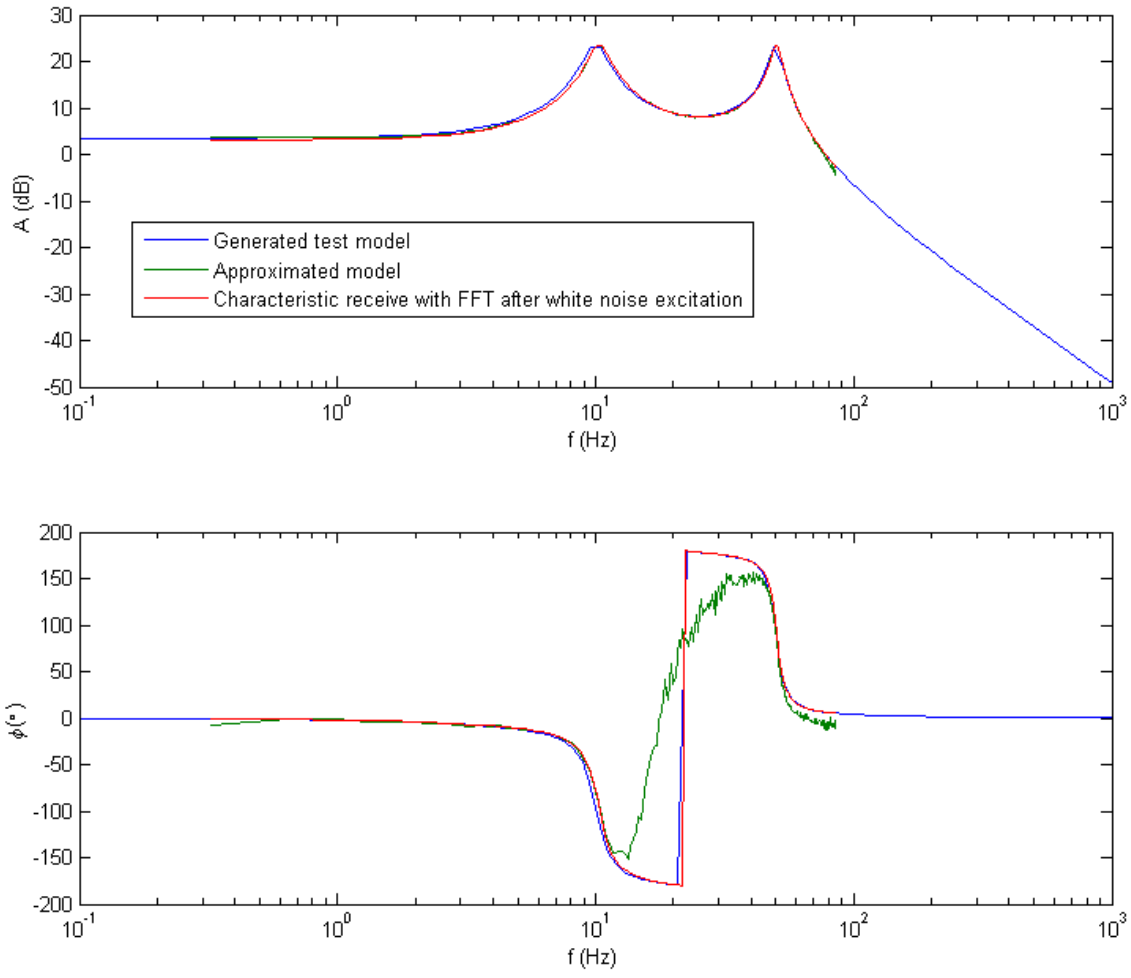

Figure 5.13: Frequency characteristic: validation of algorithm

Now we can use our measured values to create a model of our cantilever beam and actuator. We calculate six transfer functions:

- Piezoelectric actuator -> Doppler laser (non-collocated setting)
- Piezoelectric actuator -> Piezoelectric sensor (collocated setting)
- Kinematic excitation source -> Doppler laser (non-collocated setting)
- Kinematic excitation source -> Piezoelectric sensor (collocated setting)
- Doppler laser (V) -> System variables (mm) (well-known output sensitivity)
- Doppler laser (V) -> Piezoelectric sensor (V)

To find the transfer function between known Doppler laser (V) and Piezoelectric sensor (V) functions we can calculate:

$$G_{\text{kinematic to piezo}} = G_{\text{kinematic to doppler}} \cdot G_{\text{doppler to piezo}} \tag{5.37}$$

, therefore:

$$G_{\text{doppler to piezo}} = \frac{G_{\text{kinematic to piezo}}}{G_{\text{kinematic to doppler}}} \tag{5.38}$$

Results can be seen in Table 5.2. Integration is made for sensors so the results are in position.

Table 5.2: Transfer function estimation

Transformation	Transfer Function	Bode plot
Piezoelectric actuator -> Doppler laser	Equation 5.39	Figure 5.14
Piezoelectric actuator -> Piezoelectric sensor	Equation 5.40	Figure 5.15
Kinematic excitation source -> Doppler laser	Equation 5.41	Figure 5.16
Kinematic excitation source -> Piezoelectric sensor	Equation 5.42	Figure 5.17
Doppler laser (V) -> System variables (mm)	Equation 5.43	-
Doppler laser (V) -> Piezoelectric sensor (V)	Equation 5.44	Figure 5.18

$$G_{\text{piezo to doppler}} = \frac{0.0006239s}{0.01326^2 s^2 + 2 \cdot 0.01326 \cdot 0.01746s + 1} - \frac{0.00003s}{0.0028^2 s^2 + 2 \cdot 0.0028 \cdot 0.04s + 1} \tag{5.39}$$

$$G_{\text{piezo to piezo}} = \frac{0.00075s}{0.01326^2 s^2 + 2 \cdot 0.01326 \cdot 0.0225s + 1} + \frac{0.00005s}{0.002947^2 s^2 + 2 \cdot 0.002947 \cdot 0.04622s + 1} \tag{5.40}$$

$$G_{\text{kinematic to doppler}} = \frac{0.006865s}{0.01333^2 s^2 + 2 \cdot 0.01333 \cdot 0.02047s + 1} - \frac{0.003164s}{0.002979^2 s^2 + 2 \cdot 0.002979 \cdot 0.04428s + 1} \tag{5.41}$$

$$G_{\text{kinematic to piezo}} = \frac{0.005914s}{0.01326^2 s^2 + 2 \cdot 0.01326 \cdot 0.0227s + 1} + \frac{0.001777s}{0.002947^2 s^2 + 2 \cdot 0.002947 \cdot 0.04622s + 1} \tag{5.42}$$

$$G_{\text{doppler V to mm}} = \frac{0.001}{s} \frac{\text{mm}}{\text{V}} \tag{5.43}$$

On frequency around 42 Hz, we can see another peak with is made by torsional vibration.

From equations 5.41 and 5.42 we can obtain a transfer function to change the result from non-collocated to collocated. For a huge complexity, the transfer function is not shown here. As we can see in Figure 5.18, both resonance peaks are dampened a little bit and phase of the second mode is swapped.

$$G_{\text{doppler to piezo}} = \frac{G_{\text{kinematic to piezo}}}{G_{\text{kinematic to doppler}}} \tag{5.44}$$

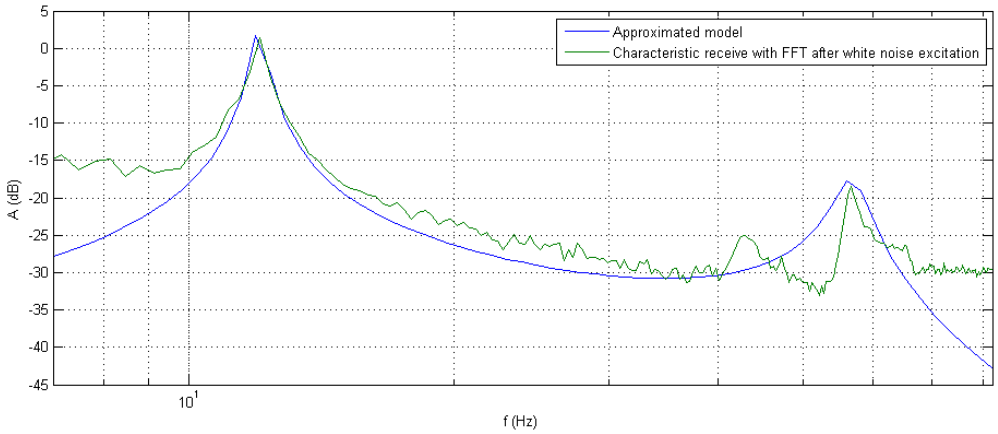

Figure 5.14: System approximation: Piezoelectric actuator -> Doppler laser

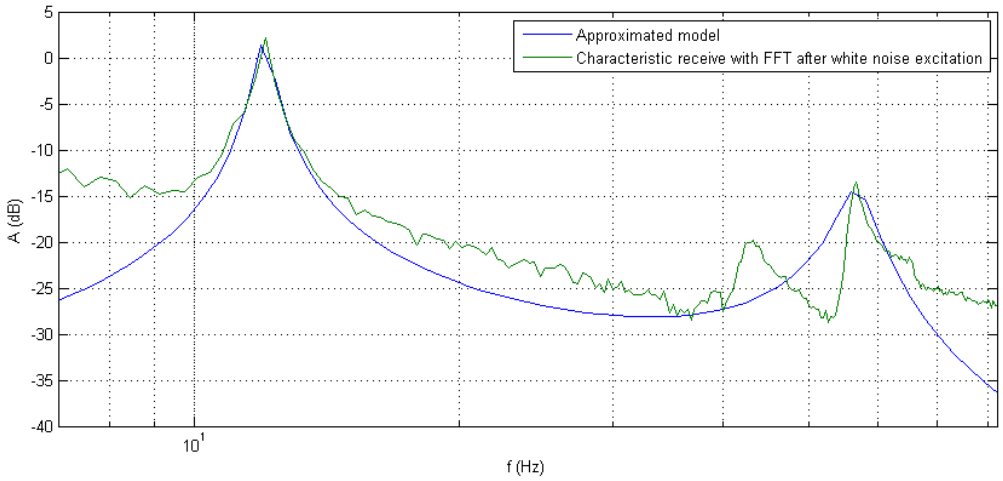

Figure 5.15: System approximation: Piezoelectric actuator -> Piezoelectric sensor

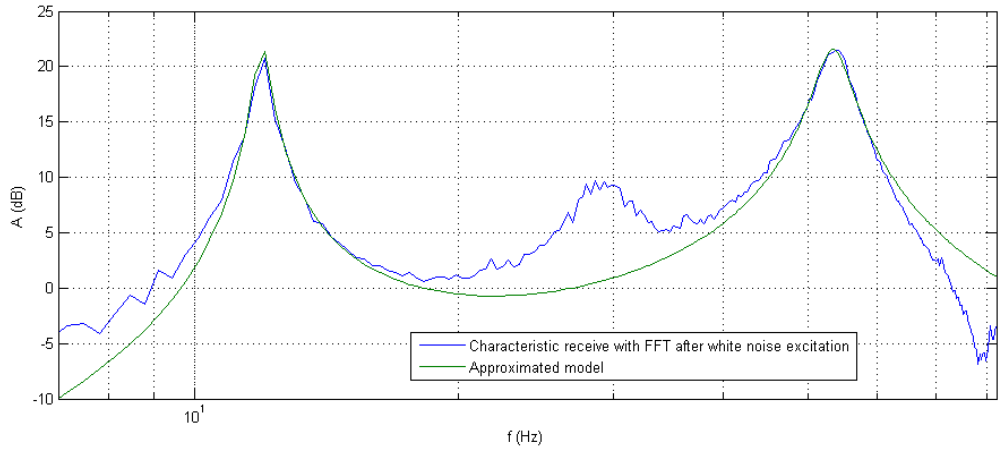

Figure 5.16: System approximation: Kinematic excitation source -> Doppler laser

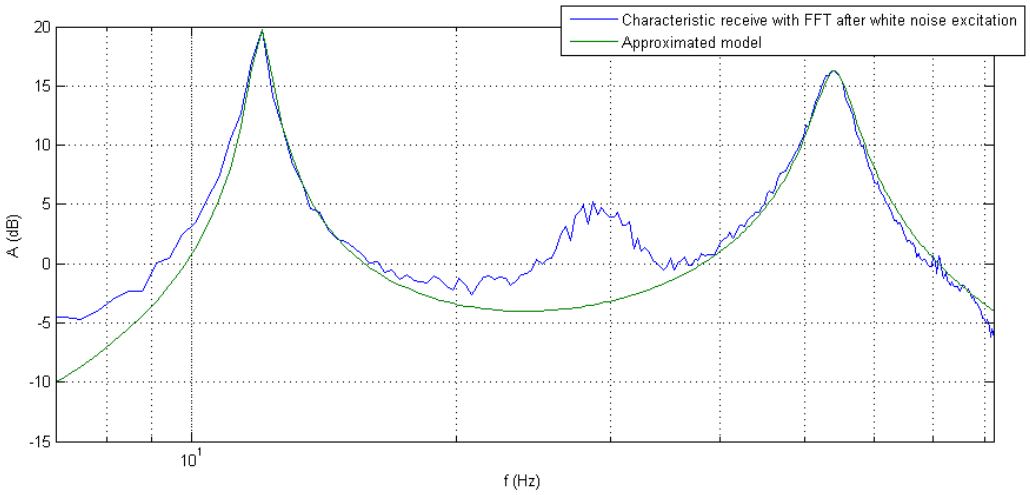

Figure 5.17: System approximation: Kinematic excitation source -> Piezoelectric sensor

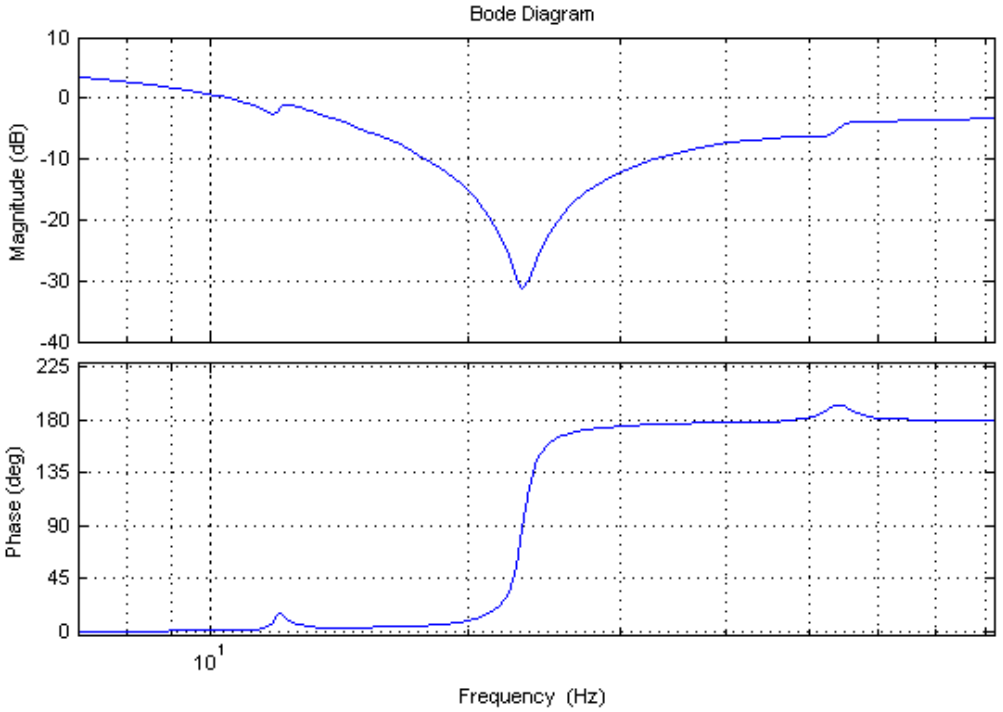

Figure 5.18: System approximation: Doppler laser (V) -> Piezoelectric sensor (V)

5.4 Simulation on the created model

In the previous chapter, we made an approximation of our real submodels. As we can see, the damping ratio and time constant is for all measurements almost same. The most accurate measurements are the measurements with kinematic excitation and doppler laser as a sensor. We use these measurements to create the simulation model. We model the system DoF separately. The equations of motion of equation 5.41 are:

$$T_1^2 \dot{x}_1(t) = k_{1,piezo} \cdot u_{piezo}(t) + k_{1,kinematic} \cdot u_{kinematic}(t) - 2\xi_1 T_1 x_1(t) - \int x_1 dt \tag{5.45}$$

$$T_2^2 \dot{x}_2(t) = k_{2,piezo} \cdot u_{piezo}(t) + k_{2,kinematic} \cdot u_{kinematic}(t) - 2\xi_2 T_2 x_2(t) - \int x_2 dt \tag{5.46}$$

$$x(t) = x_1(t) - x_2(t) \tag{5.47}$$

where equation 5.47 for non-collocated measurement. The implementation can be seen in Figures 5.19 to 5.21. The simulation model also contains the block "Real model limitation", where offset is created and saturation of the actuator is secured.

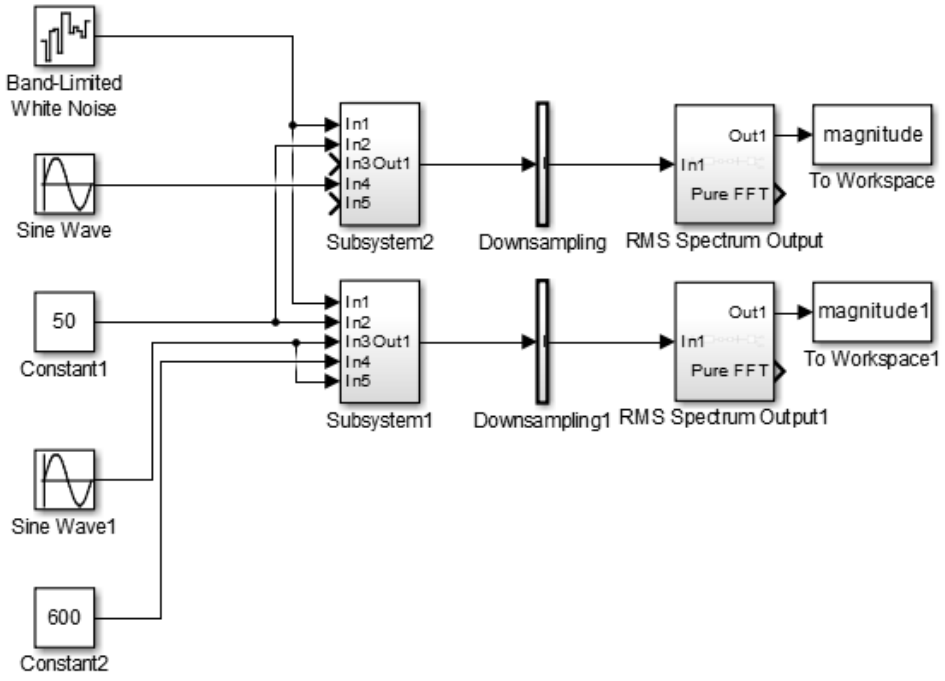

Figure 5.19: Simulink simulation model schema: corporation and measurements

The results of the simulation can be seen in 5.22. As seen, the parametric excitation on

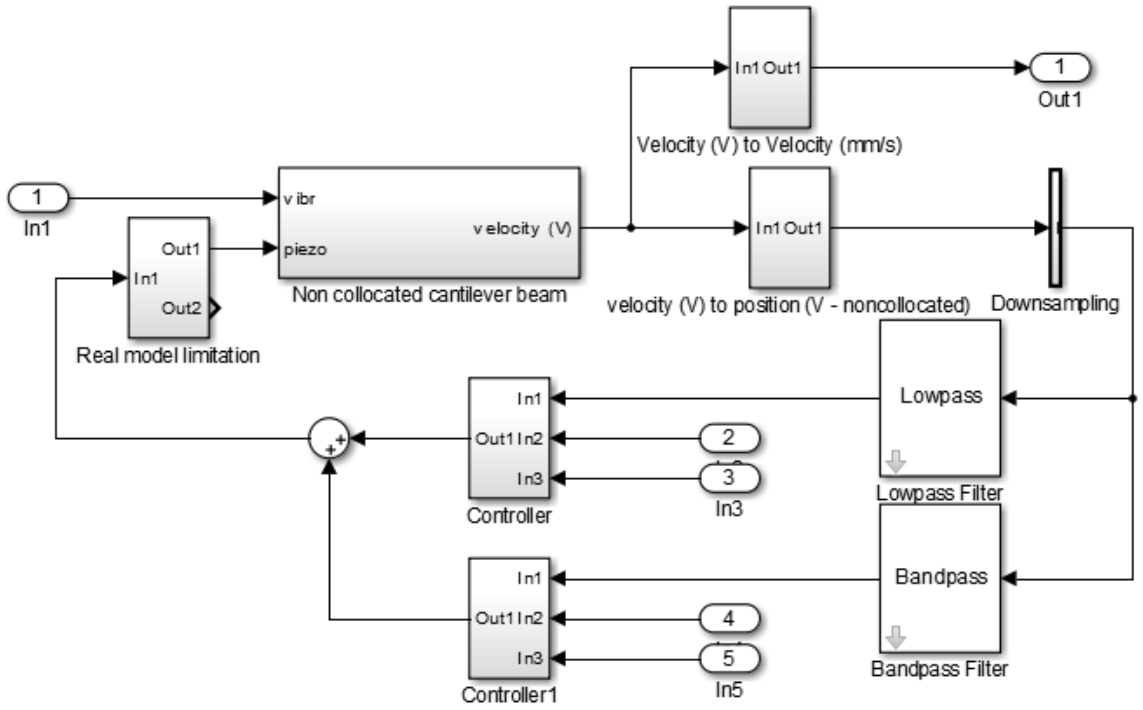

Figure 5.20: Simulink simulation model schema: measurement chain

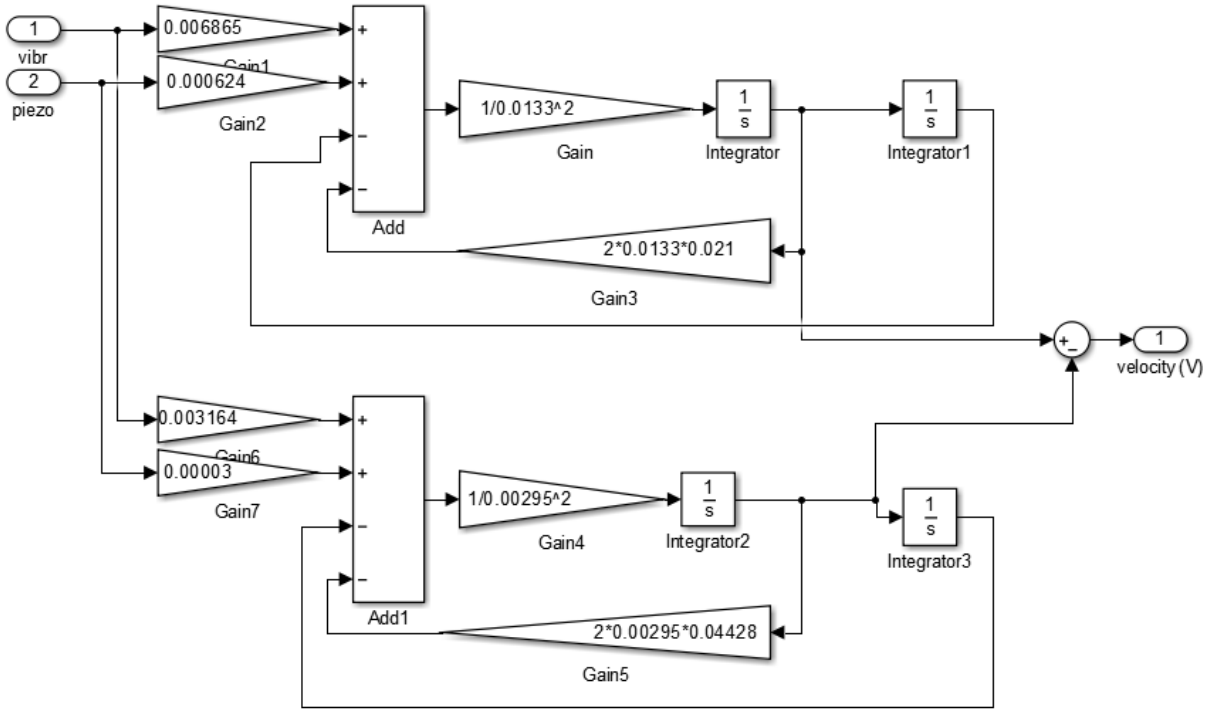

Figure 5.21: Simulink simulation model schema: Cantilever beam model

first combination resonance adds additional damping into the system. This is very useful when more linear gain cannot be used for feedback because of the output limitation. The peak is then separated into two smaller peaks. The second mode is almost not changed.

Later, the quality of the simulation model will be discussed in the practical section.

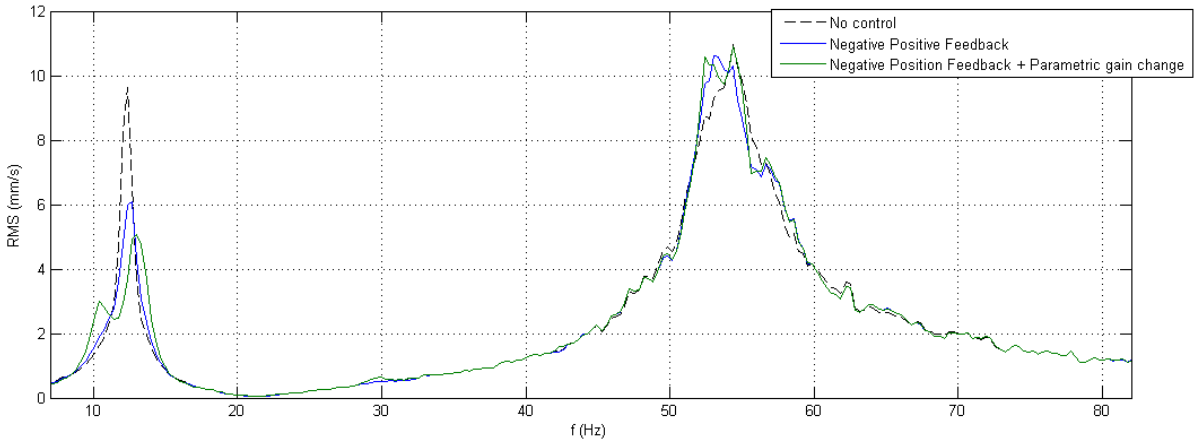

Figure 5.22: Simulink simulation results

5.5 Application of the control system on the test rig

For controller implementation, dSpace HIL system which has been discussed above is used. Because our sensors measure the velocity, it is important to make an integration. While during simulation there is no integrating error, here we need to reset the integrator from time to time to remove the direct component. Because the position is not our interest, we can simply reset the whole integrator.

For the received position feedback the proportional controller is used with harmonic change. (Figure 5.23) As we can see the change from the linear controller is minimal.

In Figure 5.24 you can see the harmonic change of regulator set to Principle resonant frequency. In this case, we work with an autonomous system which doesn't have any other excitation. Even this state is unstable, we are limited by the power of the actuator.

In Figure 5.25 you can see the harmonic change of regulator set to Combination resonant frequency. The shaker excites the beam on the natural frequency which is then effectively damped by position feedback with harmonic change.

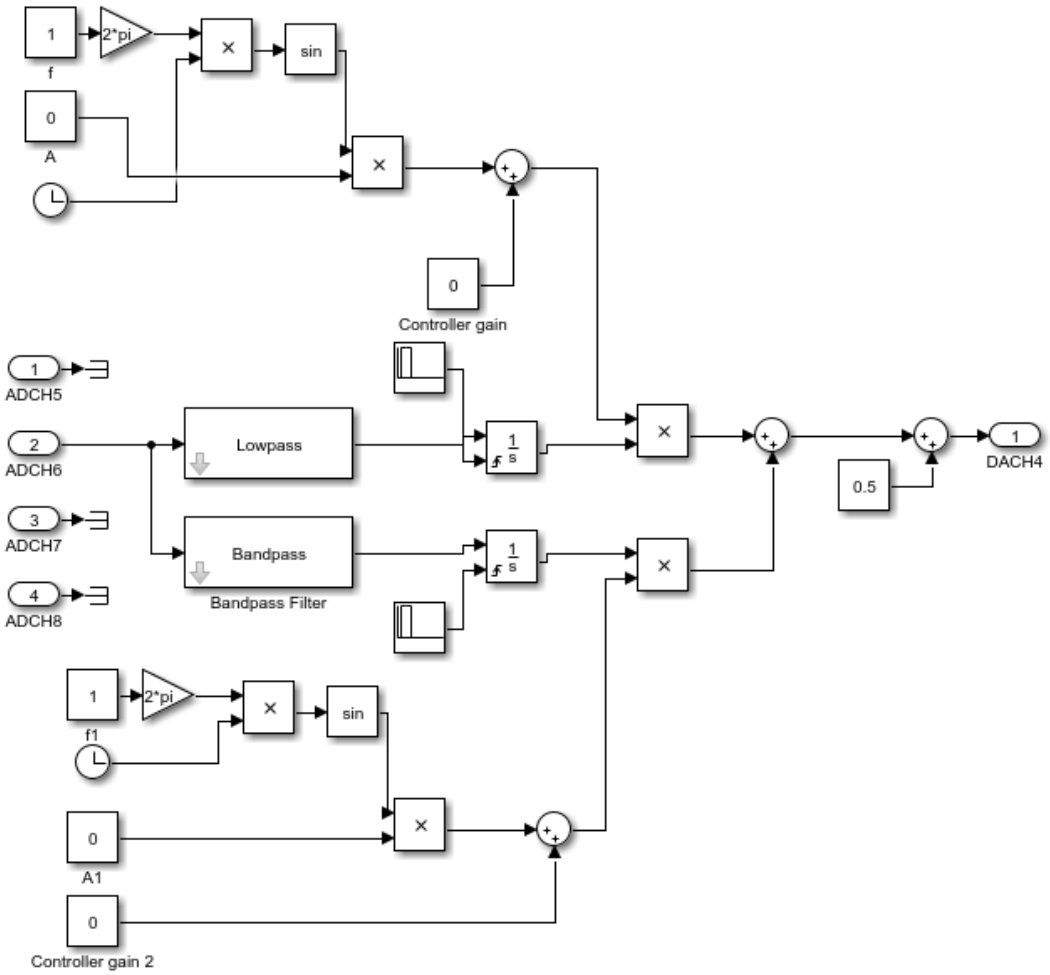

Figure 5.23: Control schema for velocity feedback

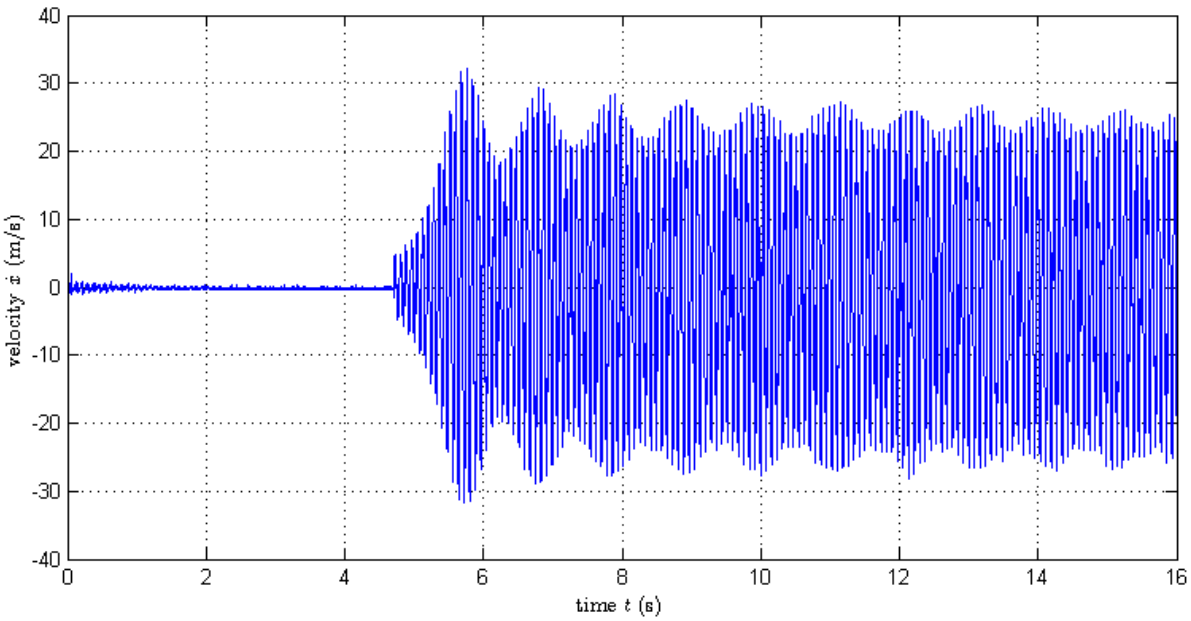

Figure 5.24: Parametricaly unstable system

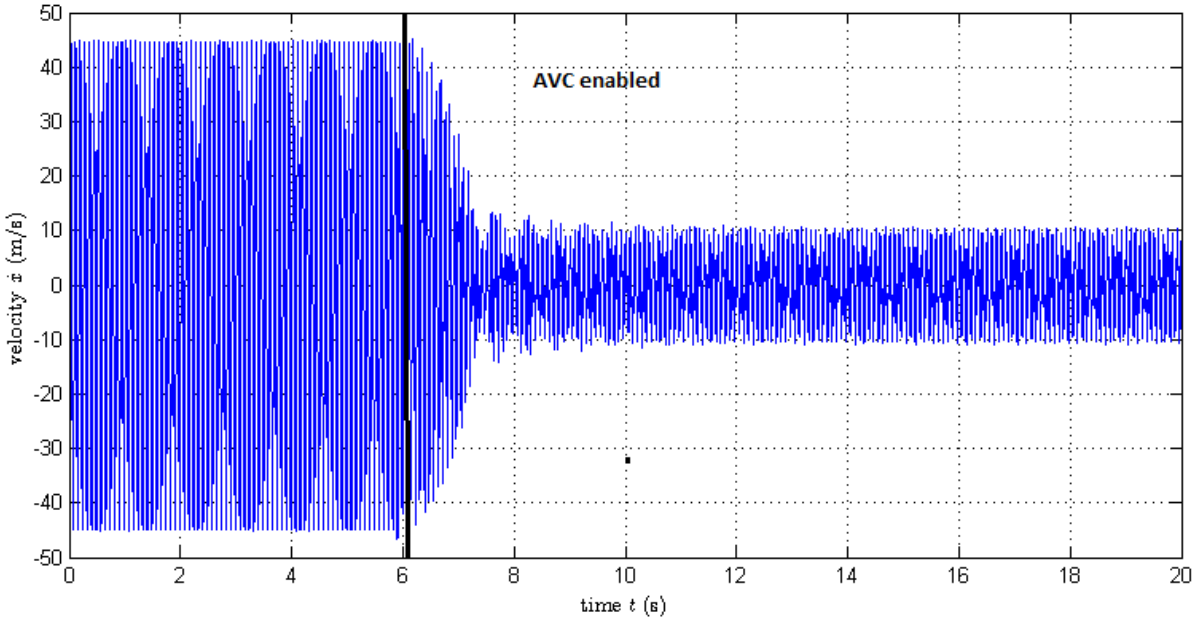

Figure 5.25: AVC with the use of parametric excitation

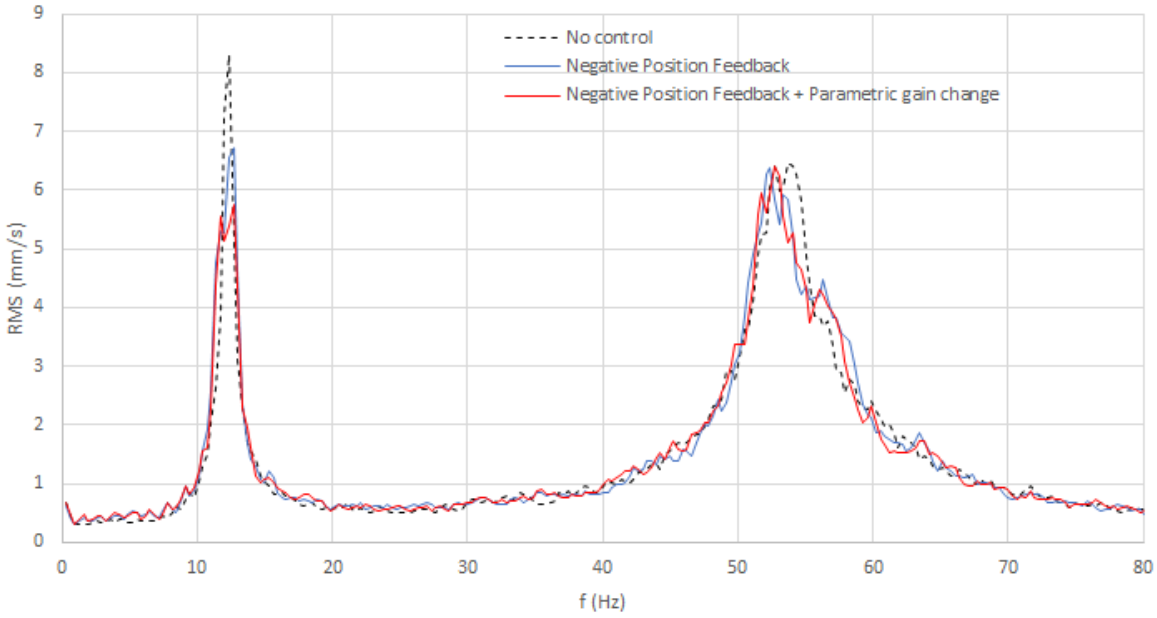

Figure 5.26: Comparision of AVC methods

To see the effect closer, the RMS spectrum is used (Figure 5.26. We can see that the results are the same as during Simulation. The first mode of resonance is slightly dampened while the second peak is almost not affected. The excitation was chosen to be the same as during the simulation. One measurement is made for 200 seconds.

Model created by frequency characteristic approximation fulfill all requirements. No theory behind the modeling needs to be calculated.

6 Conclusion and Further research

In the common active vibration structures, the velocity feedback is usually used to dampen the vibration because mechanical structure usually has a small damping coefficient. In this project, a different approach is used. **The position feedback and periodical change of the system's stiffness is used.** The Negative Position Feedback change stiffness of the system and therefore shift the resonant peak. However, the stiffness change is not made directly (via magnetorheological fluids' actuators) but by applying the force (piezoelectric actuators). The parametric excitation is **created by the harmonic change of controller's gain**. This concept **can be used in all kind of systems**.

By studying the properties of nonlinear equations of Damped Mathieu's type the instability regions are discovered and therefore designing a robust system is possible. Instability regions have the shape of tongues and their position depends on the frequency of parameter change, the amplitude and linear stiffness of the system. For basic damped Mathieu equation the frequencies can be found like:

$$\omega_n^{Pr} = \frac{2\omega_n}{n} \tag{6.1}$$

From Tondl's observation (Tondl 1991) the combination resonant frequencies of coupled multi-degree of freedom systems can be found with the equation:

$$\omega_{j\pm k,n}^{Cr} = \frac{\omega_j \pm \omega_k}{n} \tag{6.2}$$

This parametric excitation is added into the system by using a simple controller and founded resonance frequencies act as expected. Important is to notice that **response frequencies on these resonances are changed**. The energy can be found on different frequencies.

Application of parametric excitation of these frequencies for cantilever beam damping has been proven by numerical simulation (Tůma et al. 2014b). Model to practically test the influence of this approach is made the same as the simulation model for this physical model using the Gradient Descent method optimization of the frequency characteristic. Comparison of the results in Figures 5.22 and 5.26 show that created model is very accurate and can be used to make many fast tries of controlling the beam without worrying of damaging and much faster (because thousand-second measurement can be made in few seconds).

As you can see in Figures 5.25,5.22 and 5.26 this method is a **effective way to optimize the dampening of the unwanted motions**. Piezoelectric actuators are cheap, easy to install

and easy to control. The huge disadvantage of this approach is that the unstable regions are created inside the system. Also, the energy is not removed from the system but dislocated **which create non-linearity which can confuse other sensors or diagnostic experts**.

The future studies of non-linear control application are important as far as the existence of even very small non-stability regions can create big oscillations. However, by studying these condition **we are able to create passive and active methods which give us the opportunity to dampen the vibrations effectively**. As proven in this document **changing a convenient controller to controller with parametric excitation is very simple and can be used in all kinds of dynamic systems**. The procedure to design such a system can be:

1. Apply Negative Position Feedback
2. Measure or calculate Natural Frequencies
3. Check principles resonance frequencies that they can't harm you
4. Apply parametric component

I would like to thank my supervisor prof. Ing. Jiří Tůma, CSc. for his guidance, support, and inspiration. Without him, it would never be possible to finish this thesis topic which was very new for me, still belongs to topics which are not researched enough and have not been taught.

Thank you to all teacher in VSB-Technical University of Ostrava that always try to help with patience and give knowledge for students but also to all people who work on making education and research accessible for as many as possible people.

This research was supported by the SGS project No. SP2019/51 Applied Research in the Area of Machine and Process Control.

Thank you with love to my family who gives me the opportunity and friends who help me to not get crazy when I am feeling down.

Thank you for always staying beside me.

References

ŠTRAMBERSKÝ, Radek. Aktivní tlumení vibrací s použitím piezoaktuátorů typu patch [online]. Ostrava, 2016 [cit. 2018-05-08]. Dostupné z: http://hdl.handle.net/10084/115147. Bakalářská práce. Vysoká škola báňská - Technická univerzita Ostrava.

ABE, A. Vibration Control of Pendulum Via Cable Length Manipulation, in Z. Dimitrovová, J.R. de Almeida, R. Gonçalves (eds.) "Proceedings of the 11th International Conference on Vibration Problems (ICOVP-2013)", Lisbon, Portugal, 9-12 September, 2013, AMPTAC, ISBN 978-989-96264-4-7, abstrakt s. 195, článek 9 s.

DOSSING, O, Brüel Kjær. Structural Testing Part 2, 1989.

Dohnal, Fadi. (2008). Damping by Parametric Stiffness Excitation: Resonance and Anti-Resonance. Journal of Vibration and Control - J VIB CONTROL. 14. 669-688. 10.1177/1077546307082983.

DOHNAL, F. General parametric stiffness excitation–anti-resonance frequency and symmetry. Acta Mechanica, 2008, 196.1-2: 15-31.

DOHNAL, F.; TONDL, A. Induced energy transfer between vibration modes using time-periodicity. In: 11th International Conference on Vibration Problems, Lisbon, Portugal. 2013.

DWIVEDY, Dr.S. K. Nonlinear Vibrations [online]. 28-FEBRUARY-2014. Department of Mechanical Engineering Indian Institute of Technology Guwahati Guwahati - 781039, Assam, India: National Programme on Technology Enhanced Learning (NPTEL), 2014 [cit. 2018-05-08]. Dostupné z: http://nptel.ac.in/courses/112103022/1

GHANDCHI, Tehrani M. a M.K. KALKOWSKI. Active control of parametrically excited systems. Intelligent Material Systems and Structures. 2016, 27(No. 9), 28. DOI: 10.1177/1045389X15588625. ISSN 1045-389X.

MIDÉ. Piezo Protection Advantage: Product datasheet. REVISION No. 001. 2016.

NANOMOTION. Piezo-Ceramic Motors: The Piezoelectric Effect. Nanomotion: A Johnson Electric Company [online]. [cit. 2019-01-02]. Dostupné z: https://www.nanomotion.com/piezo-ceramic-motor-technology/piezoelectric-effect/

A. H. Nayfeh and D. T. Mook, Nonlinear Oscillations, Wiley, 1979

NOSKIEVIČ, Petr. Simulace systémů. 1. vyd. Ostrava: VŠB - Technická univerzita Ostrava, 1992, 217 s. ISBN 80-7078-112-2.

NOSKIEVIČ, Petr. Modelování a simulace mechatronických systémů pomocí programu MATLAB SIMULINK. 1. vyd. Ostrava: VŠB - Technická univerzita Ostrava, 2013, 83 s. ISBN 978-80-248-3231-9.

ŠURÁNEK, Pavel. Aktivní potlačování vibrací [online]. Ostrava, 2016 [cit. 2018-05-08]. Dostupné z: http://hdl.handle.net/10084/112249. Disertační práce. Vysoká škola báňská - Technická univerzita Ostrava.

ŠVARC, Ivan, Miloš ŠEDA a Miluše VÍTEČKOVÁ. Automatické řízení. Brno: Akademické nakladatelství CERM, 2007. ISBN 978-80-214-3491-2.

TONDL, Aleš. Quenching of self-excited vibrations. Prague: Academia, 1991. ISBN 8020003428 9788020003423 0444987215 9780444987211.

TONDL, Aleš. Autoparametric resonance in mechanical systems. New York: Cambridge University Press, 2000. ISBN 0521650798.

TŮMA, J. Vehicle Gearbox Noise and Vibration: Measurement, Signal Analysis, Signal Processing and Noise Reduction Measures. Wiley, Hoboken, NJ (2014), 260 pages, ISBN: 978-1-118-35941-9. (Front matter, Contents, Preface, Acknowledgements and the first 9 pages of the book on http://eu.wiley.com/WileyCDA/WileyTitle/productCd-1118359410.html)

TŮMA, J., ŠURÁNEK, P., MAHDAL, M. & BABIUCH, M. Simulation of the parametric excitation of the cantilever beam vibrations, 15th International Carpathian Control Conference (ICCC). VŠB – Technická univerzita Ostrava, Česká republika, 2014, s. 588-591. ISBN 978-147997370-5.

TŮMA, J., ŠURÁNEK, P. & MAHDAL, M., Vibration damping of the cantilever beam with the use of the parametric excitation. The 21st International Congress on Sound and Vibration, 2014, Peking, Čína. ISBN 978-163439238-9

TŮMA, J., FERFECKI, P., ŠURÁNEK, P. & MAHDAL, M. Modelování vlivu parametrického buzení na kmitání vetknutého nosníku, in Automatizace, regulace a procesy : sborník přednášek z 10. technické konference : ČVUT v Praze, Fakulta strojní, 4.5.11.2014, DIMART, 2014, s. 7-16, ISBN 978-80-903844-8-4

VÍTEČKOVÁ, Miluše a Antonín VÍTEČEK. Stavové řízení. Ostrava: VŠB - Technická univerzita Ostrava, 2015.

List of Figures

Appendix A Signal analysis

For purposes of this thesis we mostly analyze the results not in time domain but in frequency domain. Linear systems are additive and homogeneity thanks to that we can say that frequency is not changed from from input to response. (Vítečková and Víteček 2015) For nonlinear system using frequency characteristic is inaccurate because one frequency can affect other frequency. For these purposes we are going to analyze the change of the power in the system.

For mechanical structures we usually use velocity in (m/s) units. Then we use FFT (Fast Fourier Transform) algorithm. This method is well described in (Tůma 2014).

As a input signal we usually use white noise which contain all the harmonic component in the chosen band frequencies.

For FFT it is important to choose sampling frequency a number of samples for calculation. Analyzed frequency range will be:

$$f_{min} = 0 \tag{A.1}$$

$$f_{max} = \frac{f_s}{2} \tag{A.2}$$

, where f_s is sampling frequency.

The number of samples for FFT transformation give us the resolution of output graph. For making the measurement more accurate we usually use longer input measurement and average the results. If we want to see the peaks of frequencies it is good to use time window of Hamming type.

The magnitude of FFT result will be:

$$X(k) = A(k) \cdot \frac{N}{2}; \tag{A.3}$$

, where X is FFT image,
k is index of component,
$A(k)$ is amplitude of the k's component
and N is number of samples used for FFT.

We will add some physical meaning into results by scaling it into Power Spectral Density (PSD). PSD values can be calculated like:

$$PSD(k) = 2T_s \cdot \left(\frac{|X(k)|}{N}\right)^2 \cdot \frac{1}{BW} \tag{A.4}$$

, where
T_s is sample period
and BW is correction because of time window. For Hamming window $BW = 1,5$. The unit of this value is in $\frac{A^2}{(rad/s)}$. For our purpose it will be better if we scale it into dB.

$$\text{dB/ref} = 20 \cdot \log\left(\frac{PSD(k)}{ref}\right) \tag{A.5}$$

, where $PSD(k)$ is in $\frac{A^2}{(rad/s)}$ unit
and ref is a reference value based on our situation.

In listing A.1 you can see Matlab code to plot PSD graph from measured data.

```
% gathering input data for analysis
t = simout_t;
X = simout_x; % analyzed signal

% + we need to choose the length of window for FFT
lW=4096;

% Bandwidth for Hanning window
BW=1.5;

% calculating sample frequency and period
T = diff(t);
T = mean(T);
f = 1/T;

% We prepare memory to store our signal splitted into smaller pieces
nW=floor(length(t)/lW*3-2); % number of windows for averaging
XW=zeros(lW,nW); %empty matrices for data

% We put our data into windows and apply the hamming window
```

```
for k=1:nW
    XW(:,k)=(X(1+(k-1)*floor(lW/3):1+(k-1)*floor(lW/3)+lW-1)).*hann(lW);
end

% FFT transformation
%*********************************************************
FFTX=fft(XW);
FFTXconj=conj(FFTX);


% Averadging
%*********************************************************
XX=sum(FFTX.*FFTXconj,2)/nW;

% to PSD:
PSD = 2*T*abs(XX/lW).^2/BW;

% frequency vector creation in radians per second
freq=(0:(1/lW/(1/f)):((lW-1)/lW/(1/f)))*2*pi;

%we choose reference
ref = 0.01;

% Plotting the results
semilogx(freq,20*log(PSD/ref));
xlim([min(freq) max(freq)*0.5]);
xlabel('f (rad/s)')
ylabel(['PSD dB/ref ',num2str(ref),' A^2/(rad/s)'])
grid on;
```

Listing A.1: PSD graph plotting